Massachusetts Institute of Technology

Extraction of spin-asymmetries in the production of exclusive mesons with a longitudinally polarized target

Timothy B. Hayward, Harut Avakian, Maggie Kerr

November 20th, 2025

Nucleon Structure through Generalized Parton Distributions

- Generalized Parton Distributions (GPDs) unify form factors and parton distribution functions and provide a more complete 3D picture of the nucleus.
- Give access to information on the correlations between transverse position and longitudinal momentum of quarks and gluons inside the nucleus.
- Accessible experimentally through measurements of exclusive processes such as Deeply Virtual Compton Scattering (DVCS) or Deeply Virtual Meson Production (DVMP).

		Quark Polarization		
		Unpolarized (U)	Longitudinally Polarized (L)	Transversely Polarized (T)
Nucleon Polarization	U	H		$\bar{E} = 2\tilde{H}_T + E_T$
	L		$\widetilde{H}$	$\widetilde{E}_T$
	T	E	$\widetilde{E}$	$H_T, \widetilde{H}_T$

Nucleon Tomography

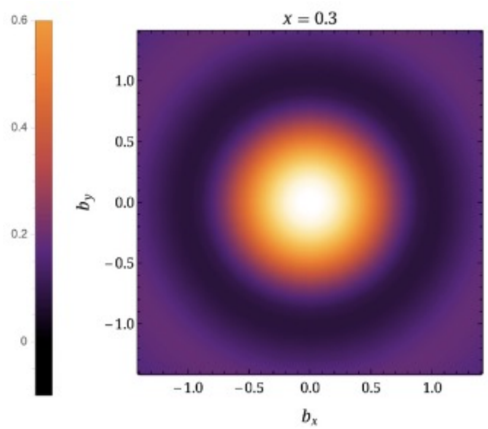

H.W. Lin, Phys. Rev. Lett. 127 (2021) 182001.

Contributions to the total nucleon spin

$$\frac{1}{2} = \frac{1}{2}\Delta\Sigma + \Delta L + \Delta G$$

X. Ji, Phys. Rev. Lett. 78,610 (1997)

1. Quark contribution; not the main contribution → spin crisis
2. Quark's orbital angular momentum, accessed through GPDs
3. Gluon spin contributions

Gravitational Form Factors

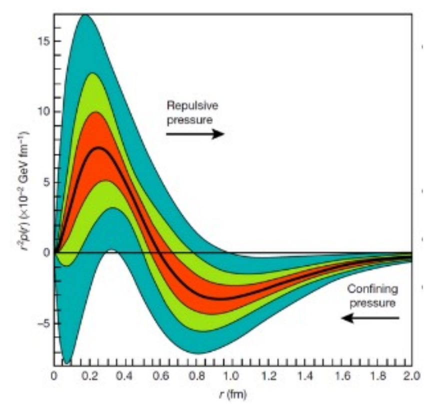

- Mass/energy distribution inside the nucleon
- Nucleon mass radius
- Shear forces and pressure distributions

V. D. Burkert et al., Nature 557.7705 (2018): 396

Nucleon Structure through (Chiral Odd) Generalized Parton Distributions

- Chiral odd GPDs encode how transversely polarized quark spins are distributed in position and momentum inside the nucleon and can be directly linked to the nucleon tensor charge and transverse-spin structure.
- Less experimentally constrained than chiral-even counterparts.
- Only appear when the hard scattering amplitude contains a chiral-odd partner (twist-3 meson distribution amplitude, transverse meson exchange, etc.)

		Quark Polarization		
		Unpolarized (U)	Longitudinally Polarized (L)	Transversely Polarized (T)
Nucleon Polarization	U	H		$\bar{E} = 2\tilde{H}_T + E_T$
	L		$\tilde{H}$	$\tilde{E}_T$
	T	E	$\tilde{E}$	$H_T, \tilde{H}_T$

Nucleon Tomography

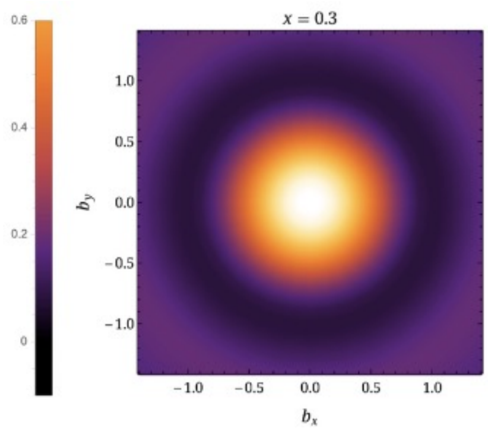

H.W. Lin, Phys. Rev. Lett. 127 (2021) 182001.

Contributions to the total nucleon spin

$$\frac{1}{2} = \frac{1}{2}\Delta\Sigma + \Delta L + \Delta G$$

X. Ji, Phys. Rev. Lett. 78,610 (1997)

1. Quark contribution; not the main contribution → spin crisis
2. Quark's orbital angular momentum, accessed through GPDs
3. Gluon spin contributions

Gravitational Form Factors

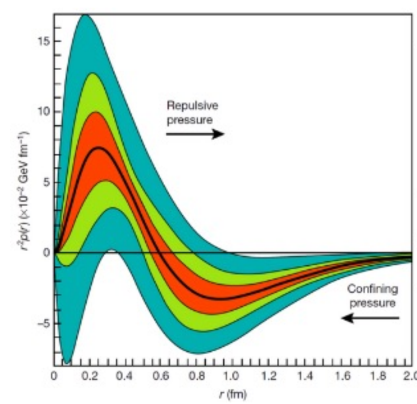

- Mass/energy distribution inside the nucleon
- Nucleon mass radius
- Shear forces and pressure distributions

V. D. Burkert et al., Nature 557.7705 (2018): 396

HERMES TSA measurements

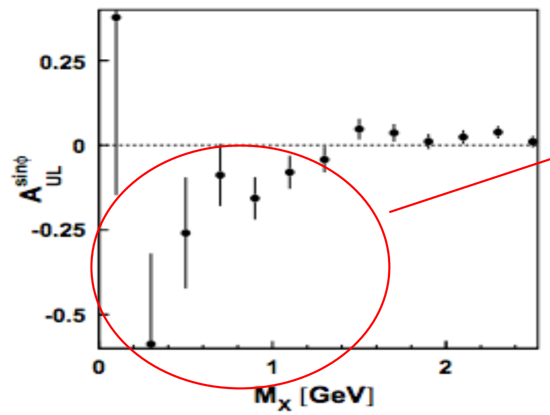

- The low statistics measurement from HERMES shows a large negative asymmetry in the exclusive region.
- CLAS(12) BSA measurements had shown positive asymmetry.
- Traditionally BSA ~ TSA.

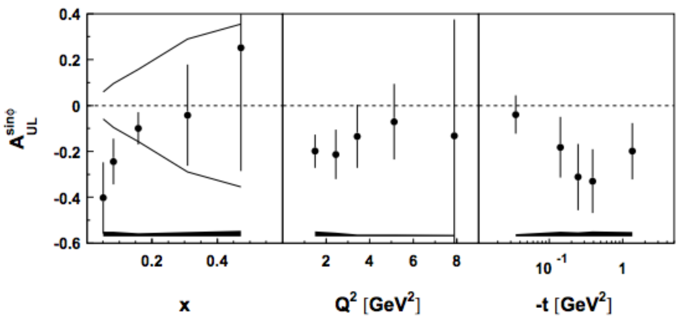

Phys.Lett.B 535 (2002) 85-92 [hep-ex/0112022]

- Similarly, measurements for exclusive π^+ and π^- were shown to have the same sign.

$$ep \to e'\pi^+ n$$

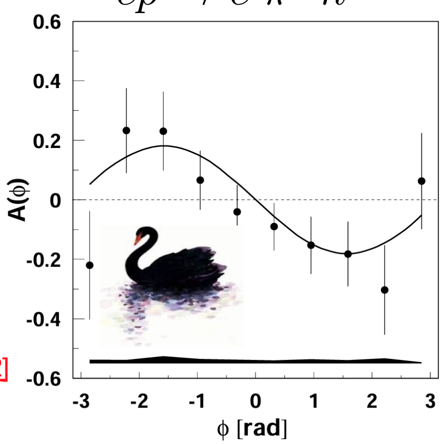

Phys.Lett.B 562 (2003) 182-192 [hep-ex/0212039]

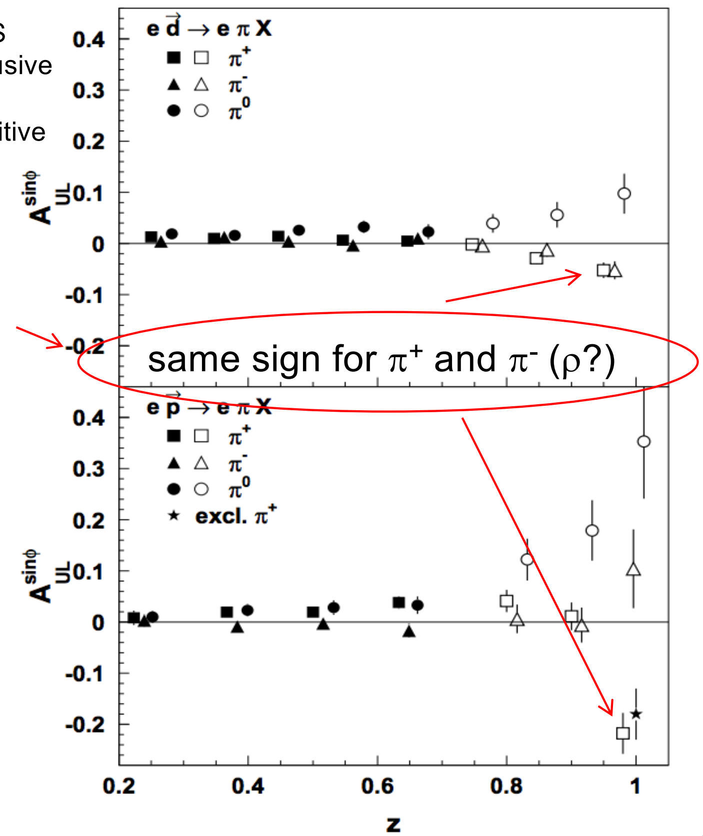

Run Group C Analysis

Period	Run Range	Beam Energy	FT	Torus	Solenoid	Coatjava Tracking	Beam Current
Su22	16043–16772	10.5473 GeV	On	−1	−1	10.0.9 (no DAF)	4 nA
Fa22	16843–17408	10.5473 GeV (16843–17065) 10.5563 GeV (17066–17408)	Off	−1	−1 (16843–17183) +1 (17185–17408)	11.1.0 (DAF)	8 nA
Sp23	17477–17811	10.5563 GeV (17477–17724) 10.5593 GeV (17725–17811)	On	−1 (17477–17768) +1 (17769–17811)	+1	11.1.0 (DAF)	4 nA

Period	Target	Total Charge (nC)	Share
Su22	NH3	3549857.7241	76.24%
	C	347844.3256	7.47%
	CH2	181529.4736	3.90%
	He	116142.5900	2.49%
	ET	460486.2692	9.89%
	Total	**4655860.3465**	
Fa22	NH3	5071114.4044	58.39%
	C	1729868.9114	19.92%
	CH2	1565074.5136	18.02%
	He	261852.4317	3.01%
	ET	57312.6648	0.66%
	Total	**8685222.9259**	
Sp23	NH3	998246.9959	45.43%
	C	331506.5461	15.09%
	CH2	431972.2728	19.68%
	He	264904.0752	12.05%
	ET	170812.0465	7.77%
	Total	**2197495.9365**	

- Make use of the full RGC inbending statistics (Su22, Fa22, Sp23).
- Dilution factor calculated via simultaneous measurements on C, CH_2, He-bath and empty target configurations.
- Target polarizations taken from combination of known A_{LL}s (elastic and DIS), P_b and D_f and solving for P_t.
- Comparison of data with both solenoid settings extensively studied with no impact on results observed.
- Leakage of tangentially polarized modulations into longitudinally polarized analysis studied with small impacts.

Asymmetry Extraction

In each kinematic bin we construct the three azimuthal asymmetries $A_{\rm LU}(\phi)$ (BSA), $A_{\rm UL}(\phi)$ (TSA), and $A_{\rm LL}(\phi)$ (DSA). The three channels are fit simultaneously using a common unpolarized denominator that carries the $\cos\phi$ and $\cos 2\phi$ modulations. Mean depolarization ratios evaluated in the bin,

$$R_{VA} \equiv \langle {\rm DepV}\rangle/\langle {\rm DepA}\rangle, \quad R_{BA} \equiv \langle {\rm DepB}\rangle/\langle {\rm DepA}\rangle, \quad R_{WA} \equiv \langle {\rm DepW}\rangle/\langle {\rm DepA}\rangle, \quad R_{CA} \equiv \langle {\rm DepC}\rangle/\langle {\rm DepA}\rangle,$$

are treated as fixed numbers and scale the corresponding harmonics. Defining the fit parameters (structure–function ratios)

$$\boldsymbol{p} = \left(C_{\rm LU},\, C_{\rm UL},\, A_{\rm LU}^{\sin\phi},\, A_{\rm UL}^{\sin\phi},\, A_{\rm UL}^{\sin 2\phi},\, A_{\rm LL},\, A_{\rm LL}^{\cos\phi},\, A_{\rm UU}^{\cos\phi},\, A_{\rm UU}^{\cos 2\phi}\right),$$

with $A_X^h \equiv F_X^h/F_{\rm UU}$, the shared denominator and the three model curves are

$$D(\phi) = 1 + R_{VA}\, A_{\rm UU}^{\cos\phi}\cos\phi + R_{BA}\, A_{\rm UU}^{\cos 2\phi}\cos 2\phi, \tag{1}$$

$$A_{\rm LU}^{\rm model}(\phi;\boldsymbol{p}) = C_{\rm LU} + \frac{R_{WA}\, A_{\rm LU}^{\sin\phi}\,\sin\phi}{D(\phi)}, \tag{2}$$

$$A_{\rm UL}^{\rm model}(\phi;\boldsymbol{p}) = C_{\rm UL} + \frac{R_{VA}\, A_{\rm UL}^{\sin\phi}\,\sin\phi + R_{BA}\, A_{\rm UL}^{\sin 2\phi}\,\sin 2\phi}{D(\phi)}, \tag{3}$$

$$A_{\rm LL}^{\rm model}(\phi;\boldsymbol{p}) = \frac{R_{CA}\, A_{\rm LL} + R_{WA}\, A_{\rm LL}^{\cos\phi}\,\cos\phi}{D(\phi)}, \tag{4}$$

where $C_{\rm LU}$ and $C_{\rm UL}$ absorb small offsets in LU and UL, respectively.

The χ^2 function is defined by letting $A_{\alpha,k}$ and $\sigma_{\alpha,k}$ denote the measured asymmetry and its statistical uncertainty in ϕ-bin k for channel $\alpha \in \{\rm LU, UL, LL\}$, evaluated at ϕ_k. The χ^2 function to be minimized in the simultaneous fit is then

$$\chi^2(\boldsymbol{p}) = \sum_k \frac{\left[A_{{\rm LU},k} - A_{\rm LU}^{\rm model}(\phi_k;\boldsymbol{p})\right]^2}{\sigma_{{\rm LU},k}^2} + \sum_k \frac{\left[A_{{\rm UL},k} - A_{\rm UL}^{\rm model}(\phi_k;\boldsymbol{p})\right]^2}{\sigma_{{\rm UL},k}^2} + \sum_k \frac{\left[A_{{\rm LL},k} - A_{\rm LL}^{\rm model}(\phi_k;\boldsymbol{p})\right]^2}{\sigma_{{\rm LL},k}^2}, \tag{5}$$

excluding any bins with vanishing $\sigma_{\alpha,k}$. All three sums share the same parameter vector $\boldsymbol{p}$, enforcing a common $\cos\phi$ and $\cos 2\phi$ denominator across the BSA, TSA and DSA.

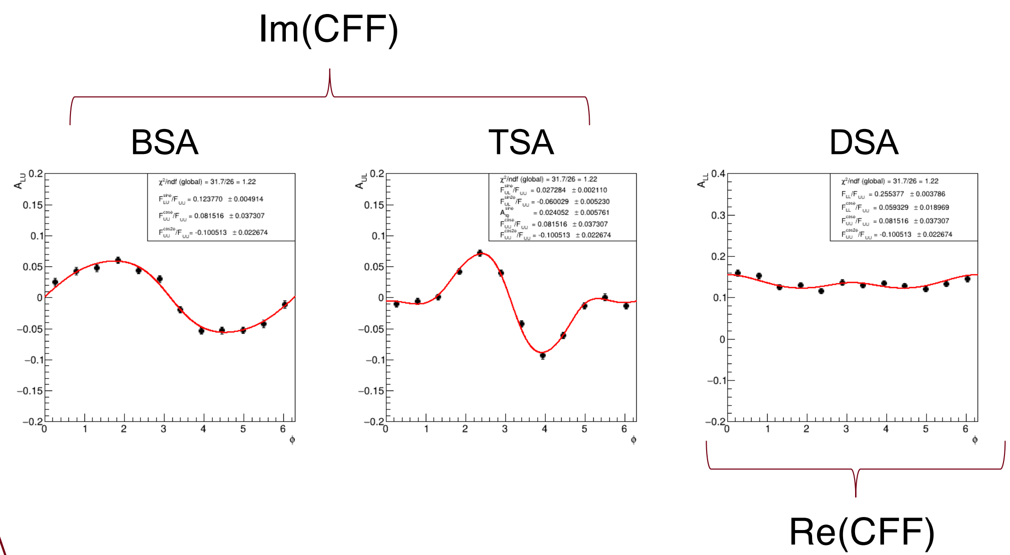

TL;DR: All five polarized modulations for BSA, TSA and DSA are extracted, with unpolarized modulations simultaneously constrained by all three histograms

CLAS12 Preliminary

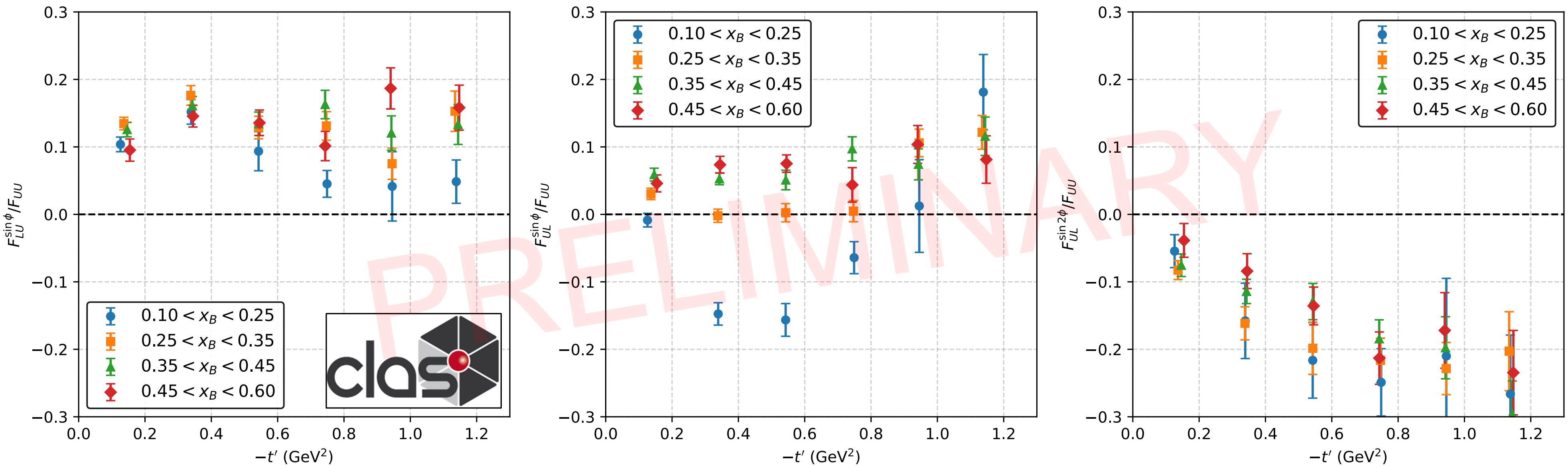

BSA

Goloskokov & Kroll, Eur. Phys. J. C **65** (2010) 137; [arXiv:0906.0460]

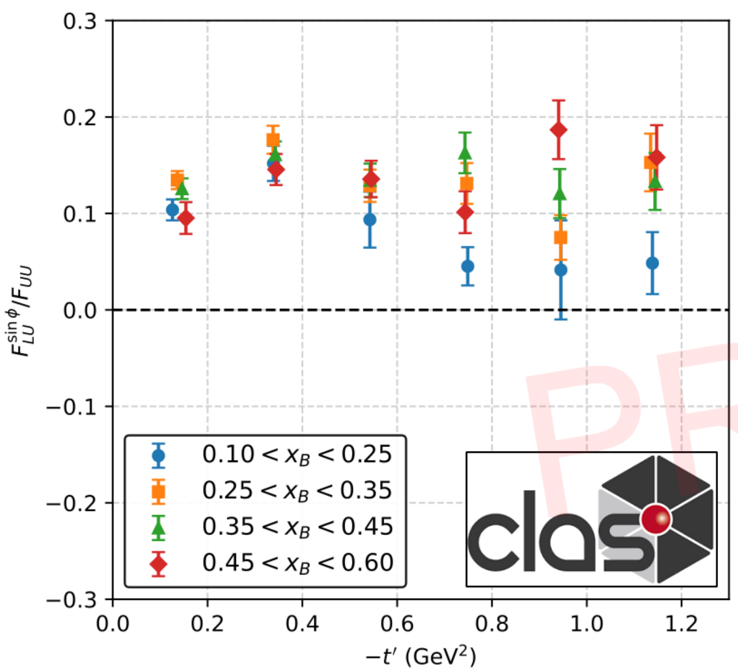

$$A_{LU}^{\sin\phi}\,\sigma_0^M = e_0^2\sqrt{1-\xi^2}\,\frac{\sqrt{-t'}}{2m}\,\mathrm{Im}\Big\{\Big[(1+\eta_M)\,\langle\bar{E}_T^M\rangle^*_{TL}+(1-\eta_M)\,\langle E_T^M\rangle^*_{TL}\Big]\langle H_{\text{eff}}^M\rangle_{LL} + \Big[\frac{t'}{2m^2}(1+\eta_M)\,\langle\tilde{H}_T^M\rangle^*_{TL} - 2\,\langle H_T^M\rangle^*_{TL}+\frac{2\xi}{1-\xi^2}\,\langle E_T^M\rangle^*_{TL}\Big]\langle E^M\rangle_{LL}\Big\}, \qquad (1)$$

η_M = -1 for pseudoscalar mesons

$$A_{LU}^{\sin\phi}\,\sigma_0^M = e_0^2\sqrt{1-\xi^2}\,\frac{\sqrt{-t'}}{2m}\,\mathrm{Im}\Big\{\underbrace{2\,\langle E_T^M\rangle^*_{TL}}_{3}\,\underbrace{\langle H_{\text{eff}}^M\rangle_{LL}}_{1} + \Big[\underbrace{-2\,\langle H_T^M\rangle^*_{TL}}_{4}+\frac{2\xi}{1-\xi^2}\,\underbrace{\langle E_T^M\rangle^*_{TL}}_{3}\Big]\underbrace{\langle E^M\rangle_{LL}}_{2}\Big\}, \qquad (3)$$

1) Helicity-conserving longitudinal amplitude built primarily from $\tilde{H}^M$, encodes the quark helicity transverse distribution
2) Nucleon helicity-flip longitudinal amplitude built from $\tilde{\mathcal{E}}^M$; describes how axial charge (helicity density) is displaced when the nucleon flips its spin
3) Describes the transverse shift of quarks with a given transverse spin inside an unpolarized nucleon, analogous to sideways shift from Sivers
4) Generalized transversity GPD (reduces to $h_1(x)$ in the forward limit), encodes information on the correlation between transversely-polarized quarks in a transversely-polarized nucleon

Twist-3 TSA

Goloskokov & Kroll, Eur. Phys. J. C **65** (2010) 137; [arXiv:0906.0460]

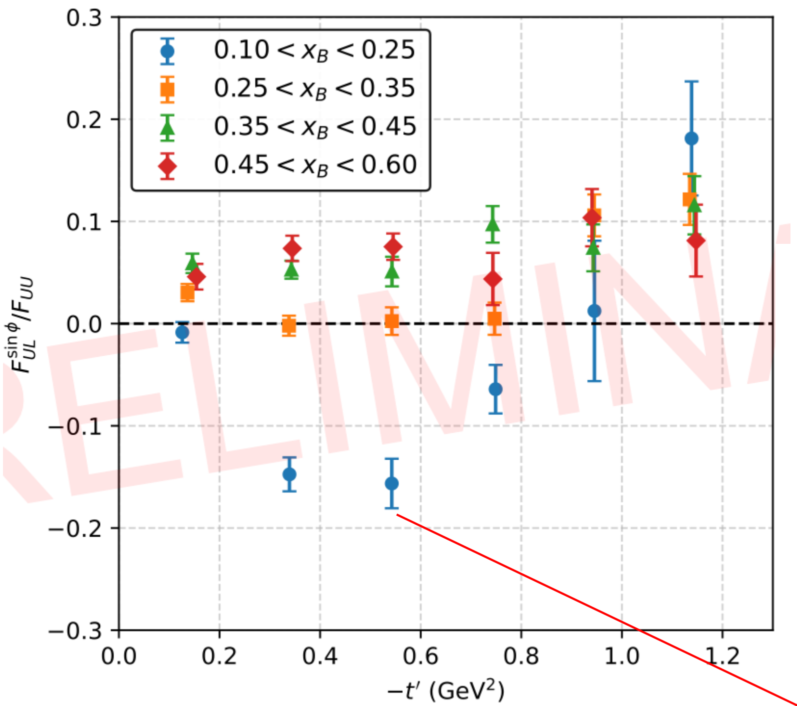

$$A_{UL}^{\sin\phi}\,\sigma_0^M = e_0^2\,\sqrt{1-\xi^2}\,\frac{\sqrt{-t'}}{2m}\,\mathrm{Im}\Big\{\Big[(1-\eta_M)\,\langle\overline{E}_T^M\rangle^*_{TL} + (1+\eta_M)\,\langle E_T^M\rangle^*_{TL}\Big]\langle H_{\text{eff}}^M\rangle_{LL}$$
$$+\Big[\frac{t'}{2m^2}(1-\eta_M)\,\langle\tilde{H}_T^M\rangle^*_{TL} - 2\,\langle H_T^M\rangle^*_{TL} + \frac{2\xi}{1-\xi^2}\,\langle E_T^M\rangle^*_{TL}\Big]\langle E^M\rangle_{LL}\Big\}. \quad (2)$$

η_M = -1 for pseudoscalar mesons

$$A_{UL}^{\sin\phi}\,\sigma_0^M = e_0^2\,\sqrt{1-\xi^2}\,\frac{\sqrt{-t'}}{2m}\,\mathrm{Im}\Big\{2\,\underbrace{\langle\overline{E}_T^M\rangle^*_{TL}}_{6}\,\underbrace{\langle H_{\text{eff}}^M\rangle_{LL}}_{1} + \Big[\frac{t'}{m^2}\,\underbrace{\langle\tilde{H}_T^M\rangle^*_{TL}}_{5} - 2\,\underbrace{\langle H_T^M\rangle^*_{TL}}_{4} + \frac{2\xi}{1-\xi^2}\,\underbrace{\langle E_T^M\rangle^*_{TL}}_{3}\Big]\,\underbrace{\langle E^M\rangle_{LL}}_{2}\Big\}. \quad (4)$$

5) Partner to H_T, akin to pretzelosity, associated with quadrupole deformation in the distribution of quark transverse spin when the nucleon is transversely polarized

6) $\overline{E} = 2\tilde{H}_T + E_T$

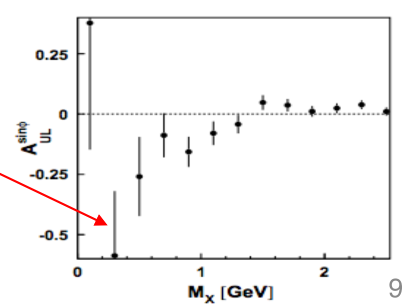

Twist-2 TSA

Goloskokov & Kroll, Eur. Phys. J. C **65** (2010) 137; [arXiv:0906.0460]

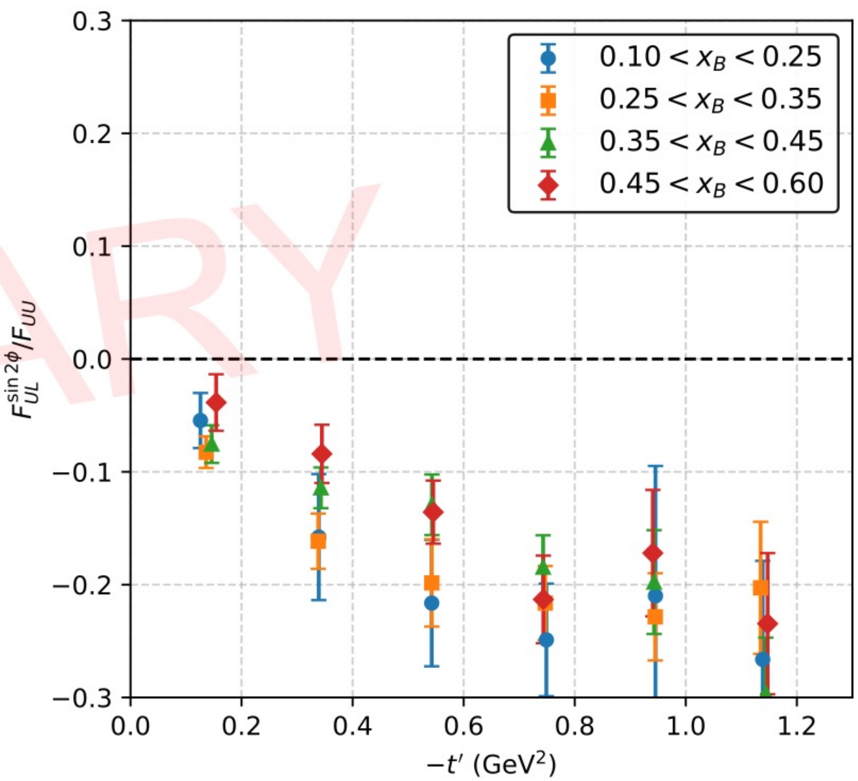

$$A_{UL}^{\sin 2\phi}\,\sigma_0^M = -\,e_0^2(1-\xi^2)\,\eta_M\,\frac{t'}{4m^2}\,\mathrm{Im}\left\{\left[\langle H_T^M\rangle^*_{TL} - \frac{\xi}{1-\xi^2}\,\langle E_T^M\rangle^*_{TL}\right]\langle \tilde{H}_T^M\rangle_{TL}\right\},$$

$$A_{UL}^{\sin 2\phi}\,\sigma_0^M = e_0^2\mathcal{P}^2\mathrm{Im}\left\{\left[\langle H_T^M\rangle^*_{TL} - \frac{\xi}{1-\xi^2}\,\langle E_T^M\rangle^*_{TL}\right]\langle \tilde{H}_T^M\rangle_{TL}\right\},$$

- The sin2ϕ TSA is TT interference, built purely from chiral-odd GPDs (as opposed to the twist-3 asymmetries being generated from interference between chiral-even and chiral-odd GPDs).
- Clear nonzero asymmetry indicates nonzero chiral-odd GPDs. In particular:

$$\tilde{H}_T^M \neq 0$$

$$H_T^M - \frac{\xi}{1-\xi^2}E_T^M \neq 0$$

$$\mathrm{phase}\left(H_T^M - \frac{\xi}{1-\xi^2}E_T^M\right) \neq \mathrm{phase}\left(\tilde{H}_T^M\right)$$

- **First observation!**
- π^+ accesses u-d isovector distribution
- Generated asymmetry is negative -- down quarks more likely found at edges of pretzel, up more like around centers (or vice versa)

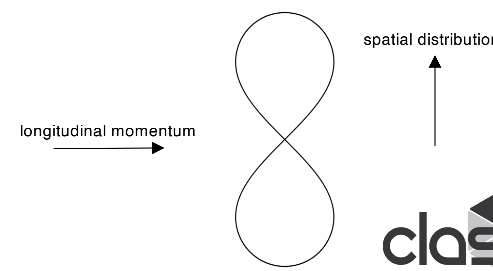

Model Comparisons to RGC Measurement

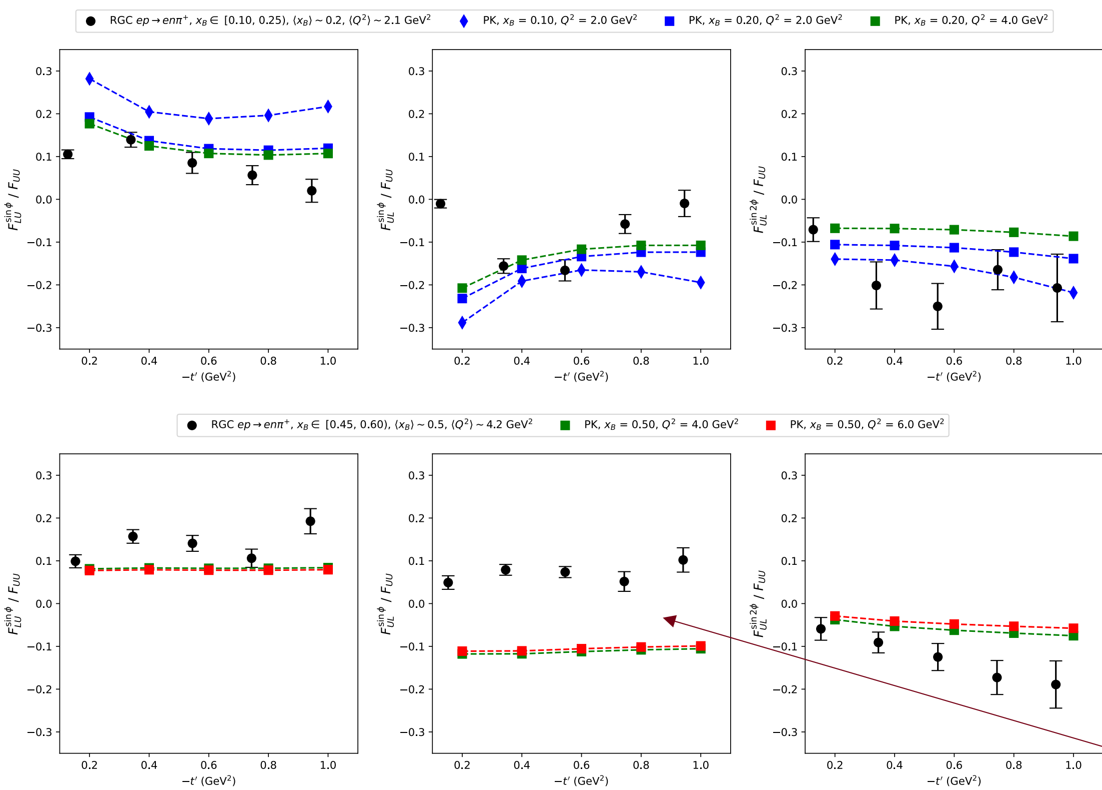

(M. Kerr, MIT)

1. $F_{LU}^{\sin\phi}$ predictions decrease with x_B while data increases with x_B.
2. $F_{UL}^{\sin\phi}$ consistently predicted negative (like HERMES) while sign flip is observed in the data in the valence region.
3. $F_{UL}^{\sin2\phi}$ always predicted negative and increasing with –t, as in data.

Goloskokov & Kroll, Eur. Phys. J. C **65** (2010) 137; [arXiv:0906.0460]

involves the helicity-flip GPD H_T [17]. As we are going to demonstrate below the data on the spin asymmetry obtained with a transversely polarized target [10] demand this contribution. With respect to the fact that we need three (almost) unknown GPDs for exclusive π^+ electroproduction we consider our analysis as a rather qualitative study, not all aspects of the data will be accommodated well. Yet we think of our work as the next step towards a comprehensive analysis of hard exclusive meson electroproduction.

Comparison between BSA and TSA

Goloskokov & Kroll, Eur. Phys. J. C **65** (2010) 137; [arXiv:0906.0460]

$$A_{LU}^{\sin\phi}\,\sigma_0^M = e_0^2\sqrt{1-\xi^2}\,\frac{\sqrt{-t'}}{2m}\,\mathrm{Im}\Big\{2\,\langle E_T^M\rangle^*_{TL}\,\langle H_{\text{eff}}^M\rangle_{LL} + \Big[-2\,\langle H_T^M\rangle^*_{TL} + \frac{2\xi}{1-\xi^2}\,\langle E_T^M\rangle^*_{TL}\Big]\,\langle E^M\rangle_{LL}\Big\}, \tag{3}$$

$$A_{UL}^{\sin\phi}\,\sigma_0^M = e_0^2\sqrt{1-\xi^2}\,\frac{\sqrt{-t'}}{2m}\,\mathrm{Im}\Big\{2\,\langle \overline{E}_T^M\rangle^*_{TL}\,\langle H_{\text{eff}}^M\rangle_{LL} + \Big[\frac{t'}{m^2}\,\langle \tilde{H}_T^M\rangle^*_{TL} - 2\,\langle H_T^M\rangle^*_{TL} + \frac{2\xi}{1-\xi^2}\,\langle E_T^M\rangle^*_{TL}\Big]\,\langle E^M\rangle_{LL}\Big\}. \tag{4}$$

It is convenient to define the overall prefactor

$$\mathcal{P} = \sqrt{1-\xi^2}\,\frac{\sqrt{-t'}}{2m}, \tag{5}$$

and express the observables as

$$A_{LU}^{\sin\phi}\,\sigma_0^M = e_0^2\mathcal{P}\,(\mathcal{C}+\mathcal{D}_{LU}), \qquad A_{UL}^{\sin\phi}\,\sigma_0^M = e_0^2\mathcal{P}\,(\mathcal{C}+\mathcal{D}_{UL}), \tag{6}$$

where the common contribution is

$$\mathcal{C} = \mathrm{Im}\Big\{\Big[-2\,\langle H_T^M\rangle^*_{TL} + \frac{2\xi}{1-\xi^2}\,\langle E_T^M\rangle^*_{TL}\Big]\,\langle E^M\rangle_{LL}\Big\}, \tag{7}$$

and the distinct pieces are

$$\mathcal{D}_{LU} = \mathrm{Im}\Big\{2\,\langle E_T^M\rangle^*_{TL}\,\langle H_{\text{eff}}^M\rangle_{LL}\Big\}, \tag{8}$$

$$\mathcal{D}_{UL} = \mathrm{Im}\Big\{2\,\langle \overline{E}_T^M\rangle^*_{TL}\,\langle H_{\text{eff}}^M\rangle_{LL} + \frac{t'}{m^2}\,\langle \tilde{H}_T^M\rangle^*_{TL}\,\langle E^M\rangle_{LL}\Big\}. \tag{9}$$

reminder: $\bar{E} = 2\tilde{H}_T + E_T$

- GK model predict negative A_{UL}; we mostly measure positive values with $A_{UL} \sim A_{LU}$.
- Either the GK model underpredicts the C term or over predicts the D_{UL} term. The fact that $A_{LU} \sim A_{UL}$ would seem to indicate the C term dominates.
- Because the $A_{UL}\sin 2\phi$ is predicted well (which contain H_T, E_T and $\tilde{H}_T$), the logical conclusion is that E^M_{LL} is being underestimated.

$$\boxed{\begin{aligned} c^{\mathrm{I}}_{1,\mathrm{TP}-} \;&\propto\; -\frac{M}{Q}\Im\mathrm{m}\Big\{\frac{t}{4M^2}\Big[(2-x_B)F_1\mathcal{E} - 4\frac{1-x_B}{2-x_B}F_2\mathcal{H}\Big] \\ &+\; x_B\xi\Big[F_1(\mathcal{H}+\mathcal{E}) - (F_1+F_2)(\tilde{\mathcal{H}} + \frac{t}{4M^2}\tilde{\mathcal{E}})\Big]\Big\}, \end{aligned} \quad (11)}$$

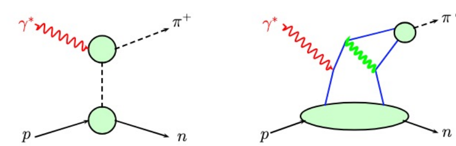

Figure 1: The pion pole (left) and the handbag (right) contribution to electroproduction of positively charged pions.

The pion pole contribution, see Fig. 1, with the residue ρ_π and pion mass m_π, will be discussed in the next section in some detail. In constrast to other work [12, 13, 14, 15] but in view of the fact that we take into account the full pion form factor and not just its perturbative contribution, we write the pion pole contributions and those from $\widetilde{E}^{(3)}$ separately, i.e. our $\widetilde{E}^{(3)}$ only represents the non-pole contribution of the full GPD. For large Q^2, $\rho_\pi \propto 1/Q^2$ so that

Comparisons to and lessons from exclusive π^-

- Exclusive π^- ($en \rightarrow ep\pi^-$) allows for additional systematic studies by detecting the recoil proton (as opposed to the unobserved neutron in exclusive π^+).
- Remarkable agreement between missing baryon peaks between RGA/RGC (H_2 and NH_3) and RGB/RGC (D_2 and ND_3).
- Comparison of A_{LU} between RGA/B and RGC shows good agreement indicating relatively nuclear effects.

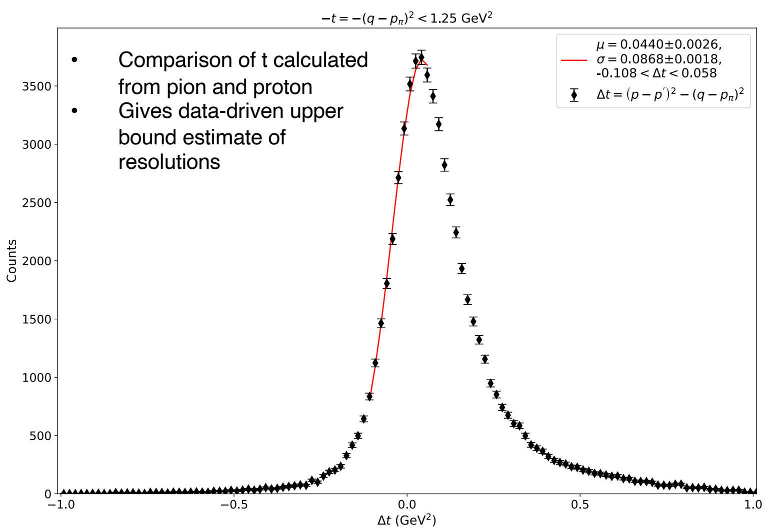

(M. Kerr, MIT)

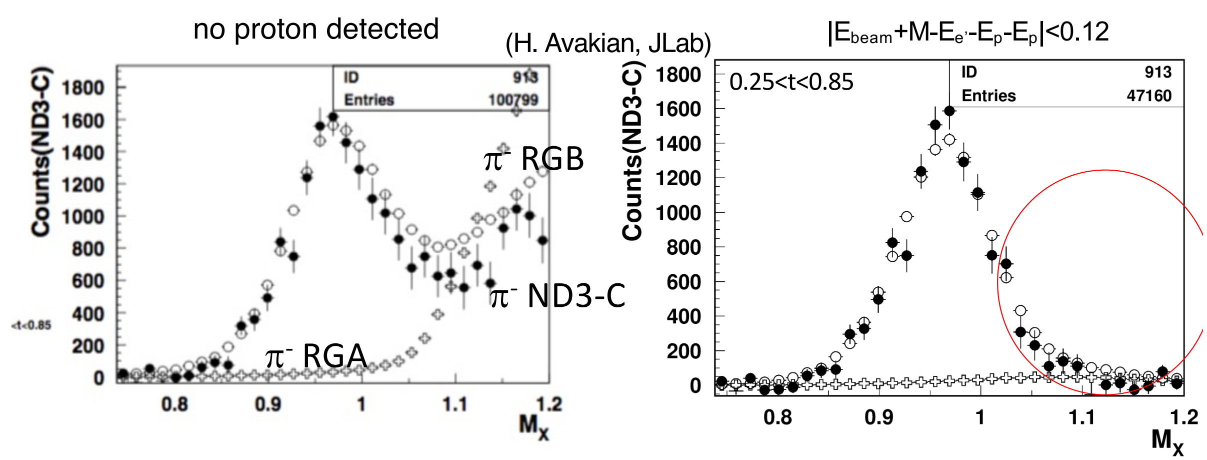

detection of proton allows for removal of background

Comparison of exclusive A_{UL}

- Exclusive π^- SSAs extracted for the first time.
- Large negative SSAs for both pions are consistent with each other.
- Consistency indicates a common source for both exclusive reactions (pion pole term?).

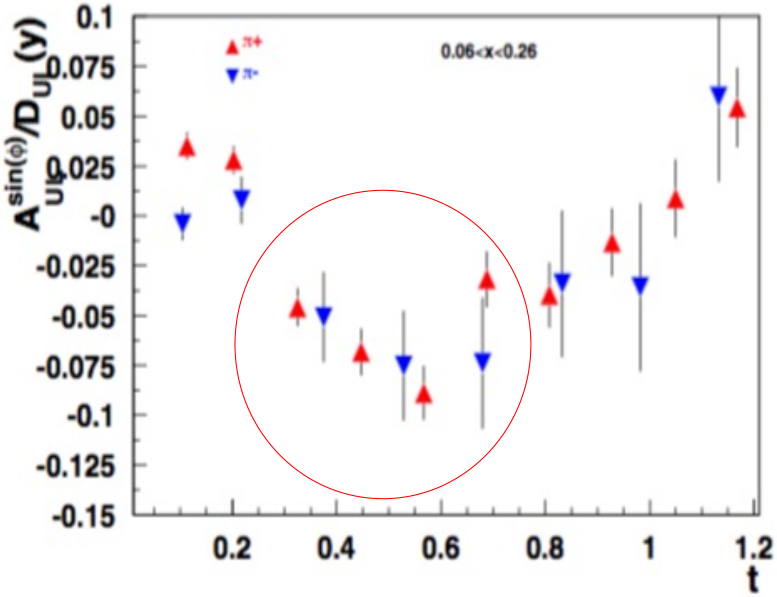

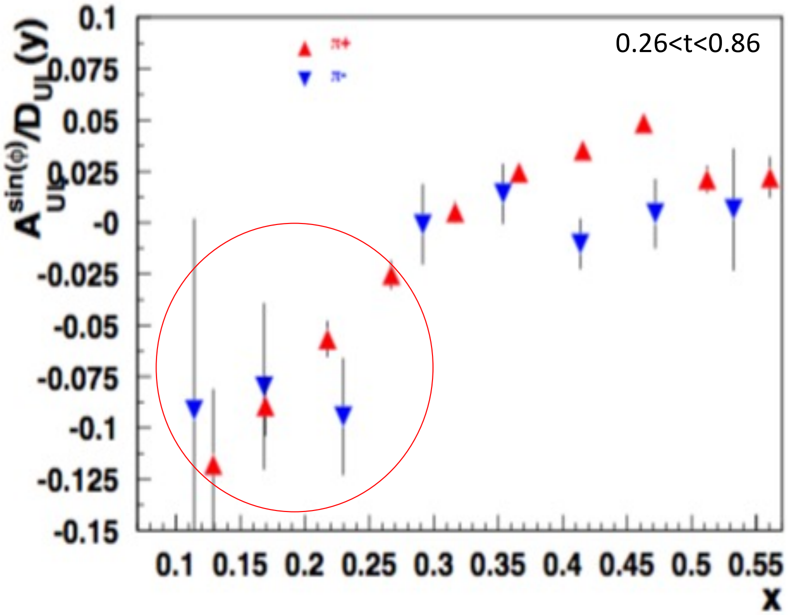

(H. Avakian, JLab)

Conclusions

- The analysis of exclusive π^+ production off NH_3 is nearly complete:
    1. Observation of negative $A_{UL}\sin\phi$ for low x_B by HERMES is confirmed.
    2. First confirmation of nonzero $A_{UL}\sin2\phi$ is observed (TT interference: chiral-odd GPDs, in particular $\tilde{H}_T^M$, confirmed nonzero!).
    3. Rich structure function extraction (5+ modulations) and comparison with predictions of GK model predictions allow for deep phenomenological study.
- Comparison between exclusive π^+ off NH_3 and exclusive π^- off ND_3, where the additional detection of the recoil proton enables detailed systematic studies and clean up of background, is ongoing. Similar behavior observed.
- π^+ and π^- target-spin asymmetries observed to be nearly identical.

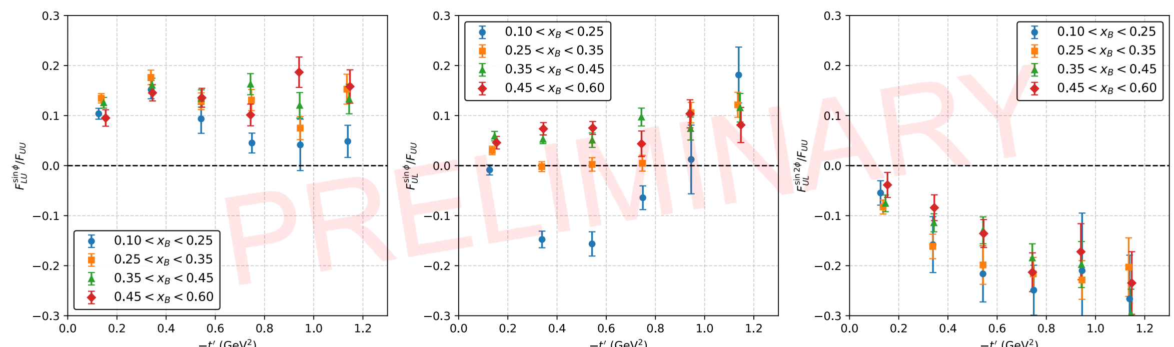

Back up

Spin Asymmetries in Deeply Virtual Meson Production

drives a sideways (dipole) shift of transversely polarized quarks in transverse plane; first moment gives anomalous tensor magnetic moment

$\mathcal{M}_{\lambda_M \lambda'_N;\lambda_\gamma \lambda_N}$

(meson helicity, final nucleon helicity; virtual photon helicity, initial nucleon helicity

		Quark Polarization		
		Unpolarized (U)	Longitudinally Polarized (L)	Transversely Polarized (T)
Nucleon Polarization	U	H		$\bar{E} = 2\widetilde{H}_T + E_T$
	L		$\widetilde{H}$	$\widetilde{E}_T$
	T	E	$\widetilde{E}$	$H_T, \widetilde{H}_T$

observable	dominant interf.	representative amplitudes	low t' behavior	relevant GPDs
$A_{UL}^{\sin\phi}$	LT	$\mathrm{Im}[\mathcal{M}^*_{0+,++}\mathcal{M}_{0-,0+}]$	$\propto \sqrt{-t'}$	$\widetilde{H},\ \widetilde{E};\ \ H_T,\ \overline{E}_T$
$A_{UL}^{\sin 2\phi}$	TT	$\mathrm{Im}[\mathcal{M}^*_{0+,++}\mathcal{M}_{0-,-+}]$	$\propto -t'$	$H_T,\ \overline{E}_T, \tilde{E}$
$A_{LU}^{\sin\phi}$	LT	$\mathrm{Im}[\mathcal{M}^*_{0-,++}\mathcal{M}_{0+,0+}]$	$\propto \sqrt{-t'}$	$\widetilde{H},\ \widetilde{E};\ \ H_T,\ \overline{E}_T$
$A_{UT}^{\sin(\phi-\phi_S)}$	LL	$\mathrm{Im}[\mathcal{M}^*_{0-,0+}\mathcal{M}_{0+,0+}]$	$\propto \sqrt{-t'}$	$\widetilde{H},\ \widetilde{E}$
$A_{UT}^{\sin(2\phi-\phi_S)}$	TT	$\mathrm{Im}[\mathcal{M}^*_{0+,++}\mathcal{M}_{0-,-+}]$	$\propto -t'$	$H_T,\ \overline{E}_T$
$A_{UT}^{\sin(\phi+\phi_S)}$	TT	$\mathrm{Im}[\mathcal{M}^*_{0-,++}\mathcal{M}_{0+,++}]$	$\propto \sqrt{-t'}$	$H_T,\ \overline{E}_T$
A_{LL}	LL	$\mathrm{Im}[\mathcal{M}^*_{0-,0+}\mathcal{M}_{0+,0+}]$	$\propto \sqrt{-t'}$	$\widetilde{H},\ \widetilde{E}$
$A_{LL}^{\cos\phi}$	LT	$\mathrm{Im}[\mathcal{M}^*_{0+,++}\mathcal{M}_{0+,0+}]$	$\propto \sqrt{-t'}$	$\widetilde{H},\ \widetilde{E};\ \ H_T,\ \overline{E}_T$

Forward limit → transversity PDF (alignment of quark's transverse spin with the nucleon's transverse spin); first moment gives the tensor charge

controls a quadrupole-type distortion of transverse spin densities when quark and nucleon are transversely polarized, an "anisotropy"; related to "pretzelosity"

ties transverse quark spin to helicity transfer along the light-cone direction, "worm gear"

- Longitudinal photons at twist-2 give amplitudes sensitive to chiral-even GPDs.
- Transverse photons generate amplitudes that involve chiral-odd (transversity) GPDs at partonic twist-2 but require twist-3 meson DA.
- $A_{UL}\sin(\phi)$ is the interference of a longitudinal amplitude (built from chiral even GPDs $\tilde{H}$ and $\tilde{E}$) with transverse amplitudes $H_T, \bar{E}_T$
- $A_{UL}\sin(2\phi)$ comes from transverse-transverse interference (built purely from chiral-odd GPDs!)
- $A_{LU}\sin(\phi)$ is the same interference as AULsin(ϕ) but in different combinations and with different kinematic weights.
- $A_{UT}\sin(\phi-\phi_s)$ is pure longitudinal-longitudinal and gives nice access to $\tilde{E}$.

Introduction

- Unpolarized GPDs can be targeted in exclusive vector meson production (H, E).
- Polarized GPDs can be targeted in exclusive pseudoscalar meson production ($\tilde{H},\tilde{E}$)

$$n_M = (-1)^J P$$

J = spin (= 0 π, 1 ρ)
P = parity (= -1)

$$\eta^V = 1 \qquad \eta^P = -1$$

$$A_{LU}^{\sin\phi} = e_0^2\sqrt{1-\xi^2}\frac{\sqrt{-t'}}{2m}\mathrm{Im}\Big[(1+\eta_M)<\bar{E}_T^M>^*_{TL}<H^M_{eff}>_{LL} \boxed{-2<H_T^M>^*_{TL}<E^M>_{LL}}\Big]$$

$$A_{UL}^{\sin\phi} = e_0^2\sqrt{1-\xi^2}\frac{\sqrt{-t'}}{2m}\mathrm{Im}\Big[(1-\eta_M)<\bar{E}_T^M>^*_{TL}<H^M_{eff}>_{LL} \boxed{-2<H_T^M>^*_{TL}<E^M>_{LL}}\Big]$$

common term, likely dominates at large x

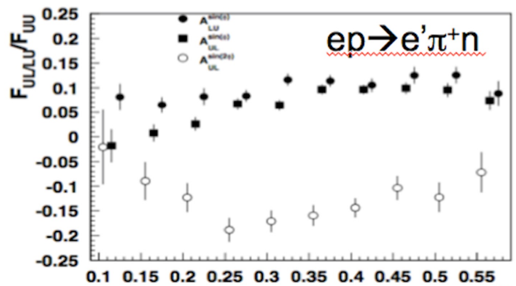

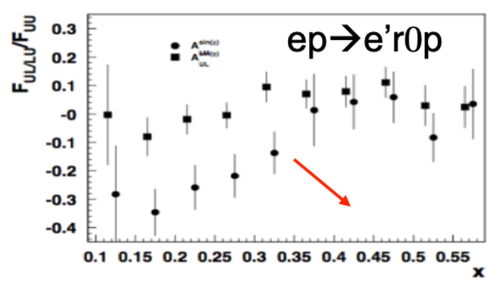

		Quark Polarization		
		Unpolarized (U)	Longitudinally Polarized (L)	Transversely Polarized (T)
Nucleon Polarization	U	H		$2\tilde{H}_T + E_T$
	L		$\tilde{H}$	$\tilde{E}_T$
	T	E	$\tilde{E}$	$H_T, \tilde{H}_T$

Twist-3 GPDs

N \ q	U	L	T
U	$\mathcal{E}_{2T}$	$\mathcal{E}'_{2T}$	$\mathcal{H}_2, \mathcal{H}'_2$
L	$\tilde{\mathcal{E}}_{2T}$	$\tilde{\mathcal{E}}'_{2T}$	$\tilde{\mathcal{H}}_2, \tilde{\mathcal{H}}'_2$
T	$\mathcal{H}_{2T}, \tilde{\mathcal{H}}_{2T}$	$\mathcal{H}'_{2T}, \tilde{\mathcal{H}}'_{2T}$	$\mathcal{E}_2, \tilde{\mathcal{E}}_2, \mathcal{E}'_2, \tilde{\mathcal{E}}'_2$

Kroll, Pion Electroproduction (2008) [arXiv:0802.0822];
Goloskokov & Kroll, Eur. Phys. J. C **65** (2010) 137.

Fully exclusive π-: A_{UL} from CLAS12 RGC

Using proton and cut $|E_{beam}+M-E_{e'}-E_p—E_\pi|<0.1$ 0.1<x<0.5

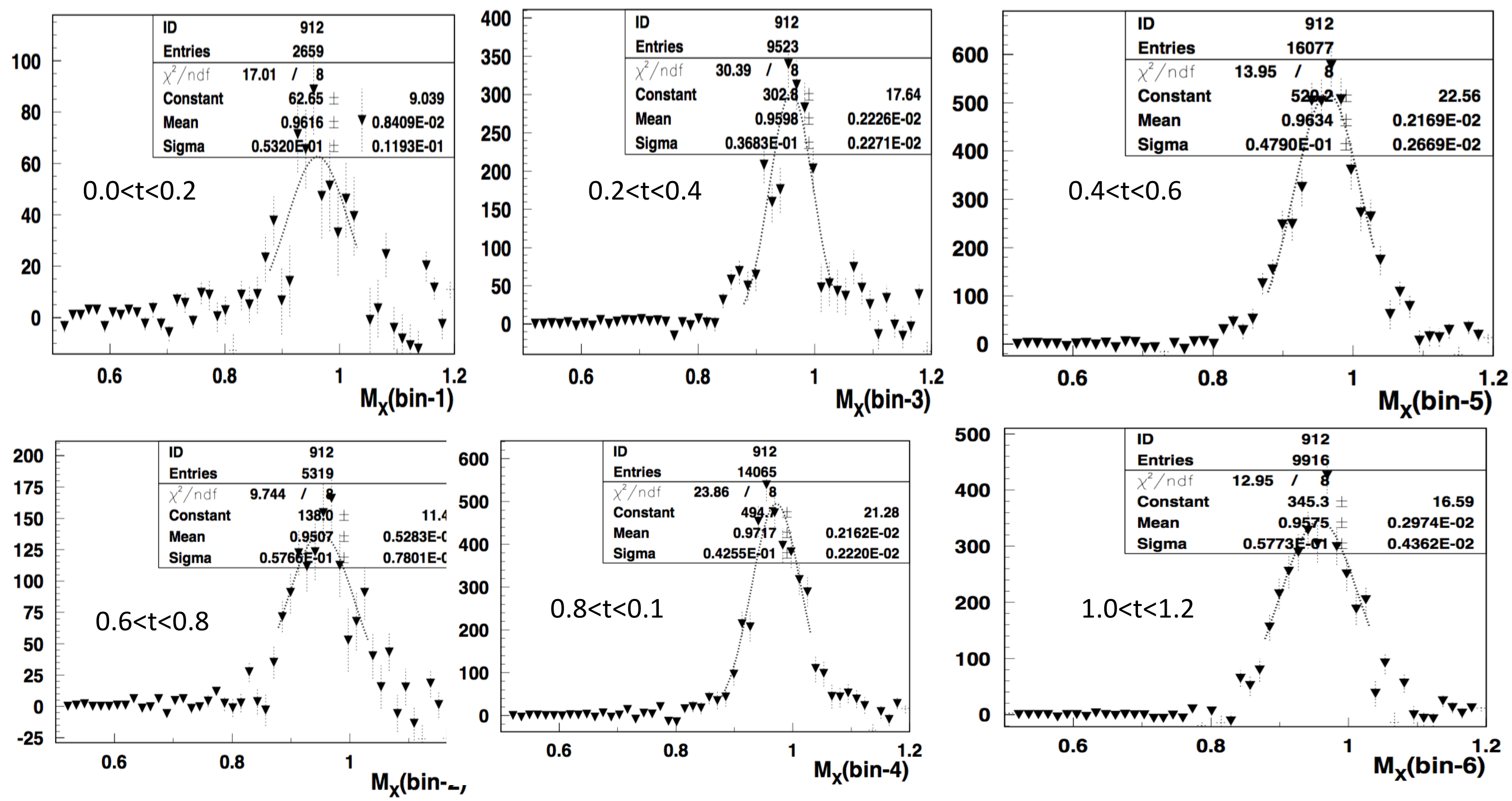

With proton detections, no major background is visible for all t

Comparison from RGC to RGA/B

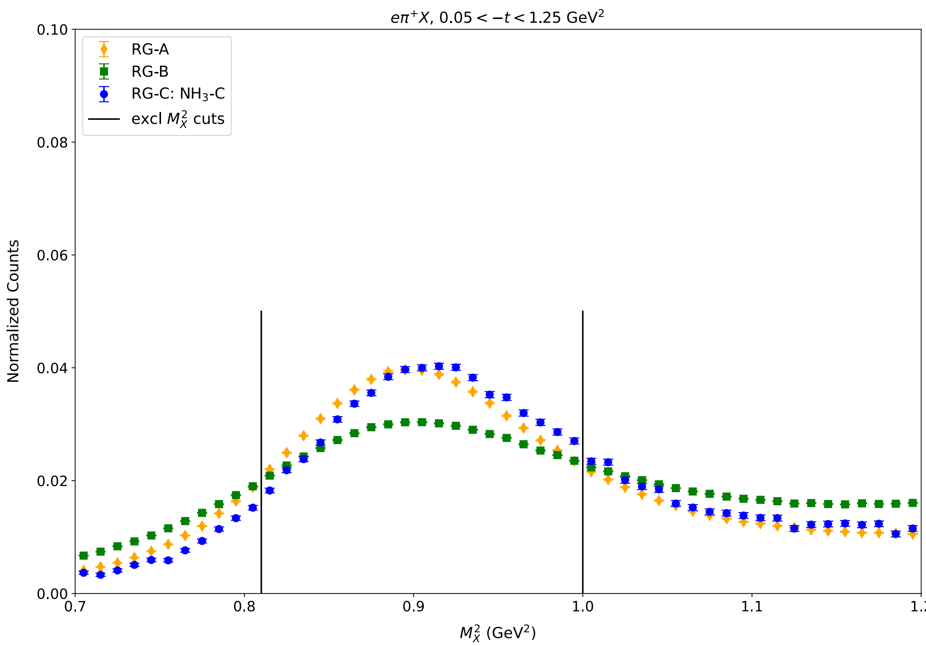

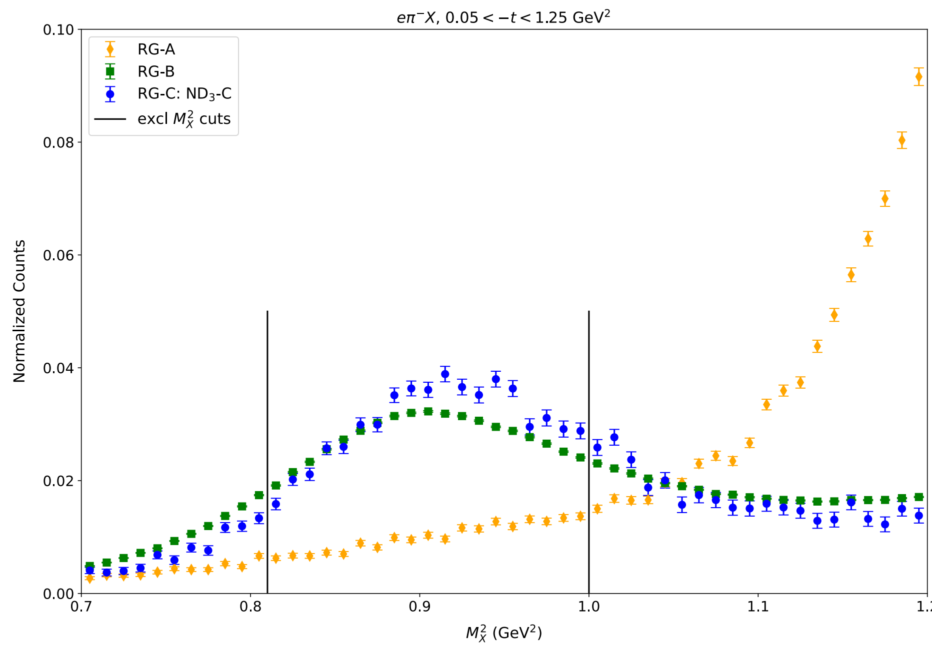

Exclusive Final State

- μ and σ are very consistent across each bin.

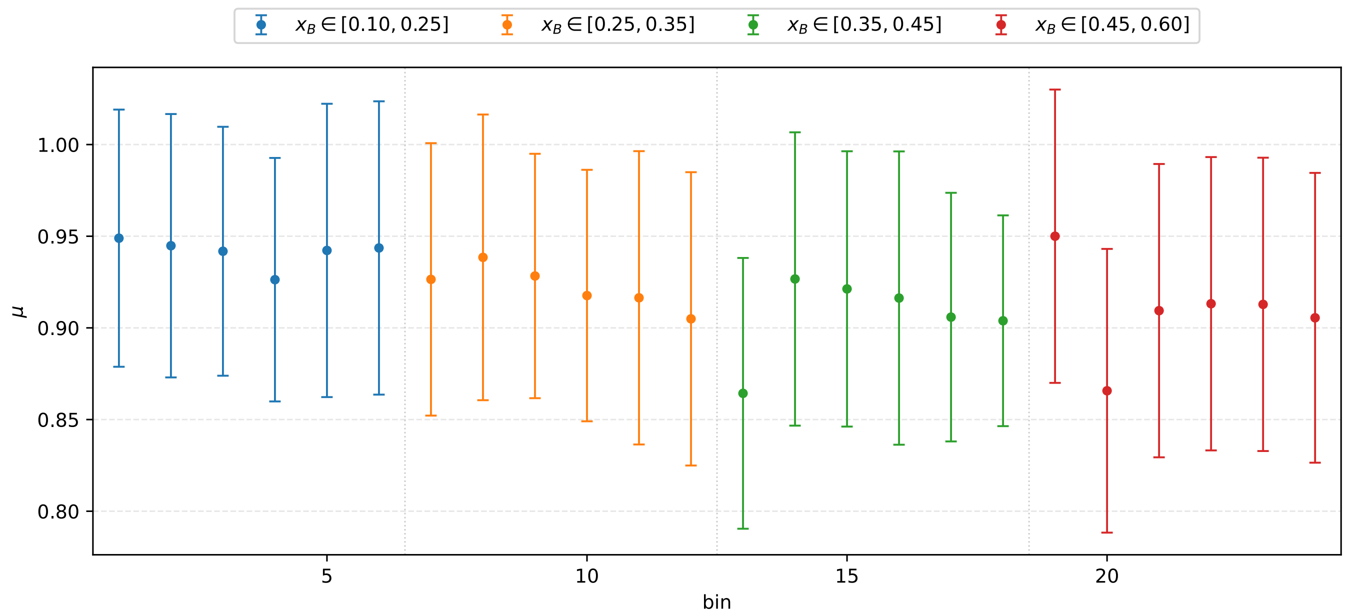

Comparison to RGA

- Charge conservation ensures that any exclusive π^+ event must have occurred with the electron scattering off a proton target.
- Very good agreement found between extracted beam-spin asymmetries from RGA Fa18 Inb and RGC Fa22 NH_3 Inb.
- Indicates that nuclear effects may be relatively small (as opposed to for example, inclusive epX).

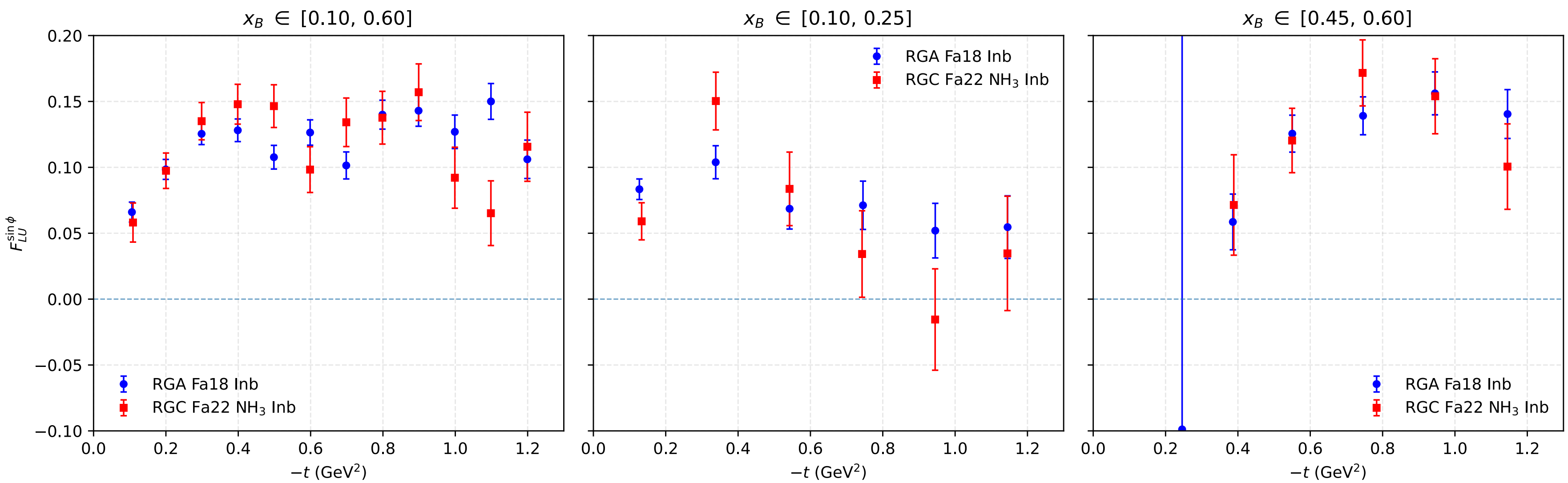

Kinematic Distributions

Binning scheme:

x_B [0.10,0.25,0.35,0.45,0.60]

-t [0.05,0.15,0.25,0.35,0.45,0.55, 0.65,0.75,0.85, 0.95,1.05,1.15,1.25]

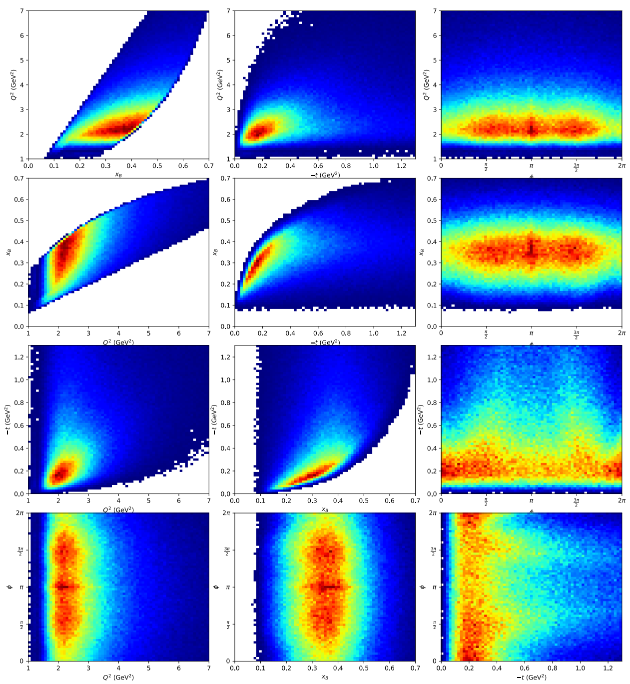

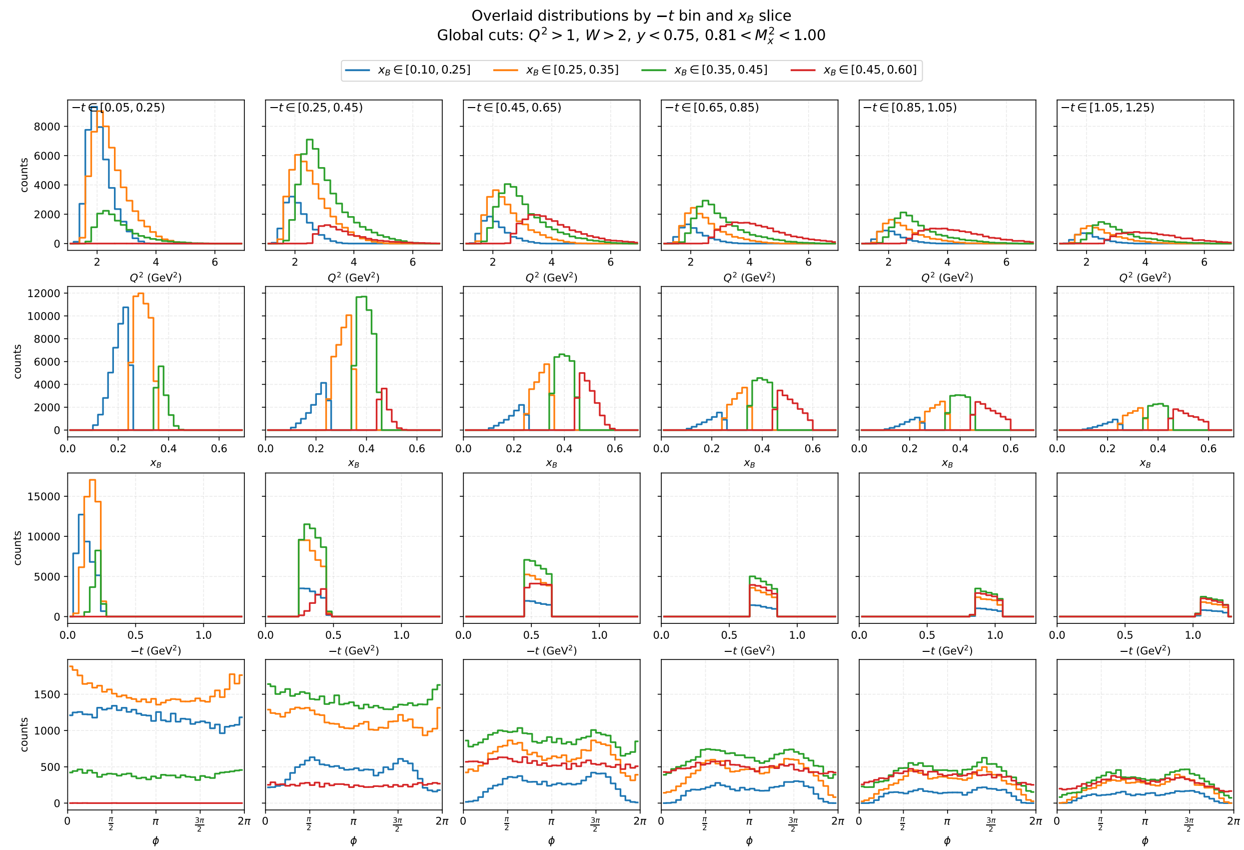

Beam Polarization

- Beam polarization determined from Moeller measurements taken through the run period.
- Su22: 83.84 +/- 0.86%
- Fa22: 83.72 +/- 0.45%
- Sp23: 80.40 +/- 0.61%

```
run number, data, polarization percentage, statistical uncertainty percentage, logbook link
only Moeller runs with charge asymmetry <2%; Hall C bleed through runs removed, adjusted Wien angles removed

RGC Su22 Inb, runs 16043-16772
140, 06/25/2022, 83.893, 1.473, https://logbooks.jlab.org/entry/4007315
163, 08/15/2022, 83.005, 1.494, https://logbooks.jlab.org/entry/4029289
164, 08/24/2022, 84.630, 1.490, https://logbooks.jlab.org/entry/4033346
Weighted Mean: 83.84 +/- 0.86(stat) +/- 0.81(sys from std); combine with 2% scale sys:
83.84 +/- 0.86(stat) +/- 2.16(sys)

RGC Fa22 Inb, runs 16843-17408
167, 09/14/2022, 86.187, 1.209, https://logbooks.jlab.org/entry/4041675
169, 09/26/2022, 81.346, 1.477, https://logbooks.jlab.org/entry/4047006
171, 10/09/2022, 87.004, 1.451, https://logbooks.jlab.org/entry/4052619
173, 10/14/2022, 82.698, 1.256, https://logbooks.jlab.org/entry/4059176
174, 10/14/2022, 80.948, 1.416, https://logbooks.jlab.org/entry/4059208
175, 10/17,2022, 84.373, 1.463, https://logbooks.jlab.org/entry/4061436
176, 10/23/2022, 82.529, 1.234, https://logbooks.jlab.org/entry/4066556
177, 10/27,2022, 85.137, 1.401, https://logbooks.jlab.org/entry/4071349
178, 11/02/2022, 83.076, 1.345, https://logbooks.jlab.org/entry/4075558
Weighted Mean: 83.72 +/- 0.45(stat) +/- 2.11(sys from std); combine with 2% scale sys:
83.72 +/- 0.45(stat) +/- 2.91(sys)

RGC Sp23 Inb, runs 17477-17811
180, 02/08/2023, 83.294, 1.494, https://logbooks.jlab.org/entry/4127008
181, 02/25/2023, 77.972, 1.464, https://logbooks.jlab.org/entry/4138705
182, 02/27,2023, 79.780, 2.280, https://logbooks.jlab.org/entry/4140187
183, 02/27/2023, 84.203, 1.499, https://logbooks.jlab.org/entry/4140437
184, 02/27/2023, 71.528, 2.097, https://logbooks.jlab.org/entry/4140449
187, 03/06/2023, 79.407, 1.492, https://logbooks.jlab.org/entry/4144176
188, 03/15/2023, 81.987, 1.476, https://logbooks.jlab.org/entry/4150249
Weighted Mean: 80.40 +/- 0.61(stat) +/- 4.25(sys from std); combine with 2% scale sys:
80.40 +/- 0.61(stat) +/- 4.70(sys)
```

Target Polarization

- N. Pilleux Wiki for elastic analysis for $P_b P_t$ extraction.
- Elastic analysis leveraging the known A_{LL} in order to determine P_t.
- Two separate DIS analyses have been performed and found to be largely consistent.

$$P_b \times P_t = \frac{\sum_{i=0}^{N_{bins}} f_i A_{th,i}(N_i^+ - N_i^-)}{\sum_{i=0}^{N_{bins}} f_i^2 A_{th,i}^2 (N_i^+ + N_i^-)}$$

$$\Delta^2_{P_b \times P_t} = \frac{\sum_{i=0}^{N_{bins}} (f_i A_{th,i})^2 (\frac{N_i^+}{FC^+} + \frac{N_i^-}{FC^-})}{(\sum_{i=0}^{N_{bins}} (f_i A_{th,i})^2 (N_i^+ + N_i^-))^2}$$

Run Period	Positive P_t	Negative P_t
RGC Su22	0.847 ± 0.037	-0.788 ± 0.037
RGC Fa22	0.848 ± 0.024	-0.836 ± 0.024
RGC Sp23	0.833 ± 0.038	-0.771 ± 0.038

- $9.5 < E_{beam}^{calc} < 11.3 GeV$
- $-0.05 < MM_{ep}^2 < 0.05 GeV^2$
- $178 < |\Phi_e - \Phi p| < 181°$
- $-0.5 < dP_p < 0.56 GeV/c$
- $-0.5 < dP_e < 0.5 GeV/c$ (difference between the expected and measured e momenta)

exclusivity selection

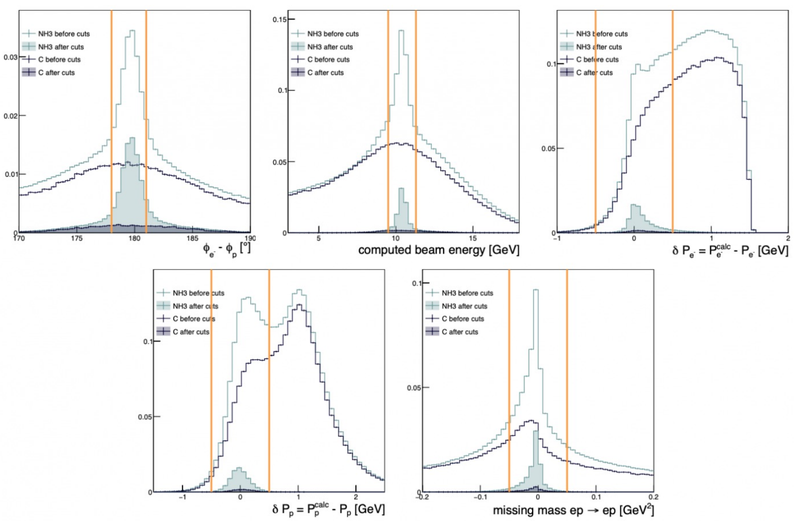

Dilution Factor Determination

[Standalone dilution factor calculation by S.E. Kuhn and D. Holmberg.]

NH/ND: Standard running with polarized e^- on the target cell filled with the polarized ammonia species of interest (NH_3 or ND_3). The total number of counts within a given bin ($\Delta Q^2, \Delta x, \ldots$) and within cuts can be written as

$$N_A = X_A f_c \left[l_F \rho_F \Delta\sigma_F + (L - l_A)\rho_{He}\Delta\sigma_{He} + l_A \rho_A \left(\frac{7}{6}\Delta\sigma_C + 3\Delta\sigma_H \right) \right] \quad (3)$$

Contribution from Al foils

Contribution from He coolant

Contribution from nitrogen in ammonia

Contribution from hydrogen in ammonia

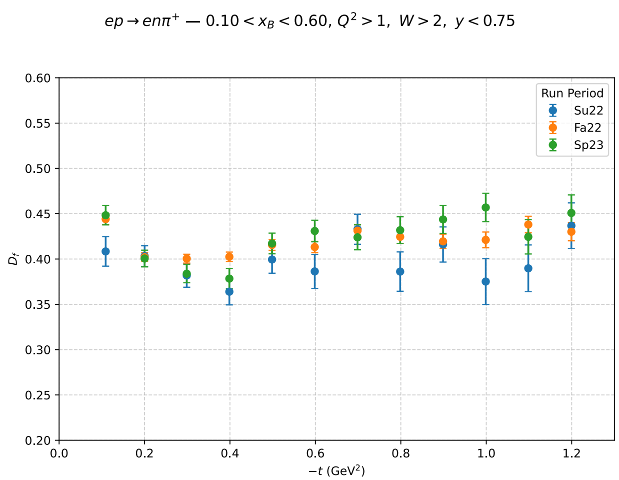

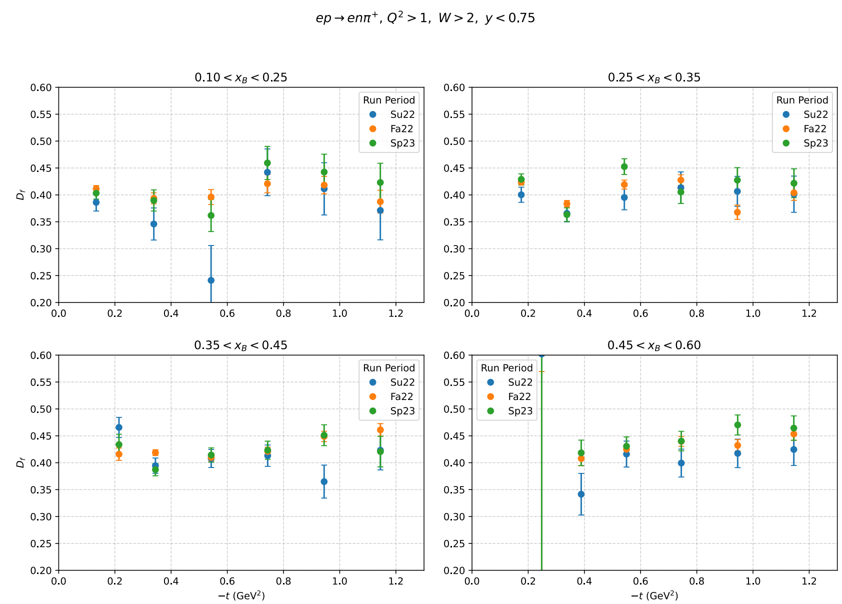

Depolarization Factors

$$A(\epsilon,y) \equiv \frac{y^2}{2(1-\epsilon)} = \frac{1}{1+\gamma^2}\left(1-y+\frac{1}{2}y^2+\frac{1}{4}\gamma^2y^2\right) \approx \left(1-y+\frac{1}{2}y^2\right),$$

$$B(\epsilon,y) \equiv \frac{y^2}{2(1-\epsilon)}\epsilon = \frac{1}{1+\gamma^2}\left(1-y-\frac{1}{4}\gamma^2y^2\right) \approx (1-y),$$

$$C(\epsilon,y) \equiv \frac{y^2}{2\,(1-\epsilon)}\sqrt{1-\epsilon^2} = \frac{y}{\sqrt{1+\gamma^2}}\left(1-\frac{1}{2}y\right) \approx y\left(1-\frac{1}{2}y\right),$$

$$V(\epsilon,y) \equiv \frac{y^2}{2\,(1-\epsilon)}\sqrt{2\epsilon(1+\epsilon)} = \frac{2-y}{1+\gamma^2}\sqrt{1-y-\frac{1}{4}\gamma^2y^2} \approx (2-y)\,\sqrt{1-y},$$

$$W(\epsilon,y) \equiv \frac{y^2}{2\,(1-\epsilon)}\sqrt{2\epsilon(1-\epsilon)} = \frac{y}{\sqrt{1+\gamma^2}}\sqrt{1-y-\frac{1}{4}\gamma^2y^2} \approx y\sqrt{1-y},$$

A. Bacchetta et al., JHEP, vol. 02, p. 093, 2007.

$$A_{LU}^{\sin\phi} = \left(\frac{W}{A}\right)\left(\frac{F_{LU}^{\sin\phi}}{F_{UU}}\right),$$

$$A_{UL}^{\sin\phi} = \left(\frac{V}{A}\right)\left(\frac{F_{UL}^{\sin\phi}}{F_{UU}}\right), \quad A_{UL}^{\sin 2\phi} = \left(\frac{B}{A}\right)\left(\frac{F_{UL}^{\sin 2\phi}}{F_{UU}}\right),$$

$$A_{LL} = \left(\frac{C}{A}\right)\left(\frac{F_{LL}}{F_{UU}}\right), \quad A_{LL}^{\cos\phi} = \left(\frac{W}{A}\right)\left(\frac{F_{LL}^{\cos\phi}}{F_{UU}}\right),$$

$$A_{UU}^{\cos\phi} = \left(\frac{V}{A}\right)\left(\frac{F_{UU}^{\cos\phi}}{F_{UU}}\right), \quad A_{UU}^{\cos 2\phi} = \left(\frac{B}{A}\right)\left(\frac{F_{UU}^{\cos 2\phi}}{F_{UU}}\right)$$

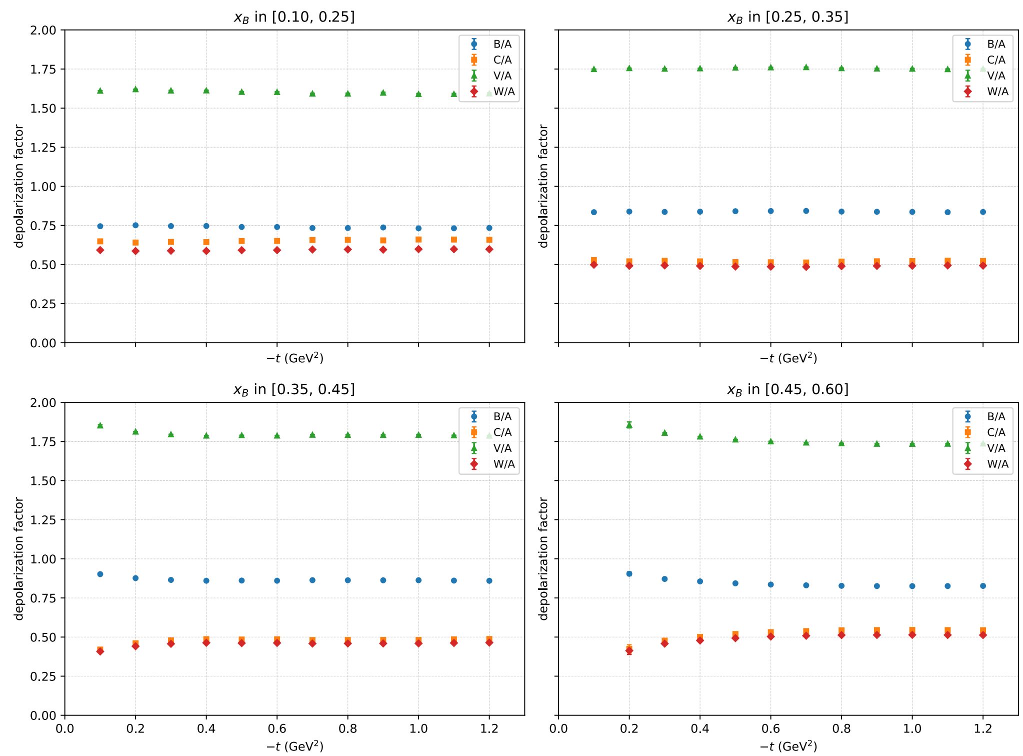

Nearly constant in –t.

Asymmetry Extraction

In each kinematic bin we construct the three azimuthal asymmetries $A_{\mathrm{LU}}(\phi)$ (BSA), $A_{\mathrm{UL}}(\phi)$ (TSA), and $A_{\mathrm{LL}}(\phi)$ (DSA). The three channels are fit simultaneously using a common unpolarized denominator that carries the $\cos\phi$ and $\cos 2\phi$ modulations. Mean depolarization ratios evaluated in the bin,

$$R_{VA} \equiv \langle \mathrm{DepV}\rangle/\langle \mathrm{DepA}\rangle, \quad R_{BA} \equiv \langle \mathrm{DepB}\rangle/\langle \mathrm{DepA}\rangle, \quad R_{WA} \equiv \langle \mathrm{DepW}\rangle/\langle \mathrm{DepA}\rangle, \quad R_{CA} \equiv \langle \mathrm{DepC}\rangle/\langle \mathrm{DepA}\rangle,$$

are treated as fixed numbers and scale the corresponding harmonics. Defining the fit parameters (structure–function ratios)

$$\boldsymbol{p} = \left(C_{\mathrm{LU}}, C_{\mathrm{UL}}, A_{\mathrm{LU}}^{\sin\phi}, A_{\mathrm{UL}}^{\sin\phi}, A_{\mathrm{UL}}^{\sin 2\phi}, A_{\mathrm{LL}}, A_{\mathrm{LL}}^{\cos\phi}, A_{\mathrm{UU}}^{\cos\phi}, A_{\mathrm{UU}}^{\cos 2\phi}\right),$$

with $A_X^h \equiv F_X^h/F_{\mathrm{UU}}$, the shared denominator and the three model curves are

$$D(\phi) = 1 + R_{VA}\, A_{\mathrm{UU}}^{\cos\phi} \cos\phi + R_{BA}\, A_{\mathrm{UU}}^{\cos 2\phi} \cos 2\phi, \tag{1}$$

$$A_{\mathrm{LU}}^{\mathrm{model}}(\phi;\boldsymbol{p}) = C_{\mathrm{LU}} + \frac{R_{WA}\, A_{\mathrm{LU}}^{\sin\phi} \sin\phi}{D(\phi)}, \tag{2}$$

$$A_{\mathrm{UL}}^{\mathrm{model}}(\phi;\boldsymbol{p}) = C_{\mathrm{UL}} + \frac{R_{VA}\, A_{\mathrm{UL}}^{\sin\phi} \sin\phi + R_{BA}\, A_{\mathrm{UL}}^{\sin 2\phi} \sin 2\phi}{D(\phi)}, \tag{3}$$

$$A_{\mathrm{LL}}^{\mathrm{model}}(\phi;\boldsymbol{p}) = \frac{R_{CA}\, A_{\mathrm{LL}} + R_{WA}\, A_{\mathrm{LL}}^{\cos\phi} \cos\phi}{D(\phi)}, \tag{4}$$

where C_{LU} and C_{UL} absorb small offsets in LU and UL, respectively.

The χ^2 function is defined by letting $A_{\alpha,k}$ and $\sigma_{\alpha,k}$ denote the measured asymmetry and its statistical uncertainty in ϕ-bin k for channel $\alpha \in \{\mathrm{LU}, \mathrm{UL}, \mathrm{LL}\}$, evaluated at ϕ_k. The χ^2 function to be minimized in the simultaneous fit is then

$$\chi^2(\boldsymbol{p}) \;=\; \sum_k \frac{\left[A_{\mathrm{LU},k} - A_{\mathrm{LU}}^{\mathrm{model}}(\phi_k;\boldsymbol{p})\right]^2}{\sigma_{\mathrm{LU},k}^2} + \sum_k \frac{\left[A_{\mathrm{UL},k} - A_{\mathrm{UL}}^{\mathrm{model}}(\phi_k;\boldsymbol{p})\right]^2}{\sigma_{\mathrm{UL},k}^2} + \sum_k \frac{\left[A_{\mathrm{LL},k} - A_{\mathrm{LL}}^{\mathrm{model}}(\phi_k;\boldsymbol{p})\right]^2}{\sigma_{\mathrm{LL},k}^2}, \tag{5}$$

excluding any bins with vanishing $\sigma_{\alpha,k}$. All three sums share the same parameter vector $\boldsymbol{p}$, enforcing a common $\cos\phi$ and $\cos 2\phi$ denominator across the BSA, TSA and DSA.

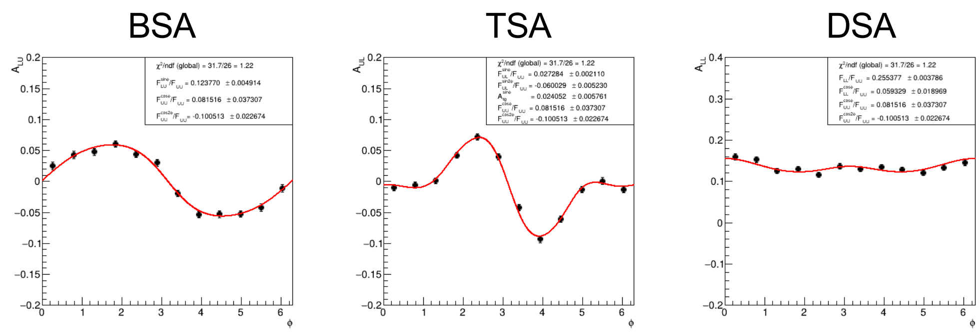

Run Group C Data Sets

Period	**Run Range**	**Beam Energy**	**FT**	**Torus**	**Solenoid**	**Coatjava Tracking**	**Beam Current**
Su22	16043–16772	10.5473 GeV	On	−1	−1	10.0.9 (no DAF)	4 nA
Fa22	16843–17408	10.5473 GeV (16843–17065) 10.5563 GeV (17066–17408)	Off	−1	−1 (16843–17183) +1 (17185–17408)	11.1.0 (DAF)	8 nA
Sp23	17477–17811	10.5563 GeV (17477–17724) 10.5593 GeV (17725–17811)	On	−1 (17477–17768) +1 (17769–17811)	+1	11.1.0 (DAF)	4 nA

Period	**Target**	**Total Charge (nC)**	**Share**
Su22	NH3	3549857.7241	76.24%
	C	347844.3256	7.47%
	CH2	181529.4736	3.90%
	He	116142.5900	2.49%
	ET	460486.2692	9.89%
	Total	**4655860.3465**	
Fa22	NH3	5071114.4044	58.39%
	C	1729868.9114	19.92%
	CH2	1565074.5136	18.02%
	He	261852.4317	3.01%
	ET	57312.6648	0.66%
	Total	**8685222.9259**	
Sp23	NH3	998246.9959	45.43%
	C	331506.5461	15.09%
	CH2	431972.2728	19.68%
	He	264904.0752	12.05%
	ET	170812.0465	7.77%
	Total	**2197495.9365**	

Run Period	**++ (M nC)**	**+− (M nC)**	**−+ (M nC)**	**−− (M nC)**
RGC Su22	0.723	1.055	0.721	1.050
RGC Fa22	1.301	1.227	1.310	1.224
RGC Sp23	0.323	0.176	0.323	0.176

QADB

- CLAS12 QADB defined in terms of “defect bits”.
- Total accumulated charges are after QA cuts.
- QADB used for all periods.
- Hall-c bleed through additionally removed.

Defect Bit Definitions

- QA information is stored for each **QA bin**, in the form of **defect bits**
  - the user needs only the run number and event number to query the QADB
- A **QA bin** is:
  - the set of events between a fixed number of scaler readouts (roughly a time bin, although there are fluctuations in a bin's duration)
  - for older QADBs, Run Groups A, B, K, and M of Pass 1 data, the QA bins were DST 5-files
- A **defect bit** is:
  - a bit (of a binary number) that is `1` if the QA bin exhibits the corresponding defect or `0` if not
  - each defect bit corresponds to a different defect, as shown in the table below
  - many defects check the value of N/F, defined as the trigger electron yield N, normalized by the DAQ-gated Faraday Cup charge F

```
// instantiate QADB
QADB qa = new QADB("latest")
qa.checkForDefect('TotalOutlier')
qa.checkForDefect('TerminalOutlier')
qa.checkForDefect('MarginalOutlier')
qa.checkForDefect('SectorLoss')
qa.checkForDefect('LowLiveTime')
qa.checkForDefect('Misc')
qa.checkForDefect('ChargeHigh')
qa.checkForDefect('ChargeNegative')
qa.checkForDefect('ChargeUnknown')
qa.checkForDefect('PossiblyNoBeam')
[ // list of runs with `Misc` that should be allowed,
  // generally empty target etc for dilution factor calculations
    5046, 5047, 5051, 5128, 5129, 5130, 5158, 5159,
    5160, 5163, 5165, 5166, 5167, 5168, 5169, 5180,
    5181, 5182, 5183, 5400, 5448, 5495, 5496, 5505,
    5567, 5610, 5617, 5621, 5623, 6736, 6737, 6738,
    6739, 6740, 6741, 6742, 6743, 6744, 6746, 6747,
    6748, 6749, 6750, 6751, 6753, 6754, 6755, 6756,
    6757,                                          // RGA runs ^
    16194, 16089, 16185, 16308, 16184, 16307, 16309, // RGC Su22 He/ET
    16872, 16975,                                  // RGC Fa22 He/ET
    17763, 17764, 17765, 17766, 17767, 17768,        // RGC Sp23 He/ET
    17179, 17180, 17181, 17182, 17183, 17188, 17189, // RICH off/partially down
    17252
].each{ run -> qa.allowMiscBit(run) }
```

Particle Identification

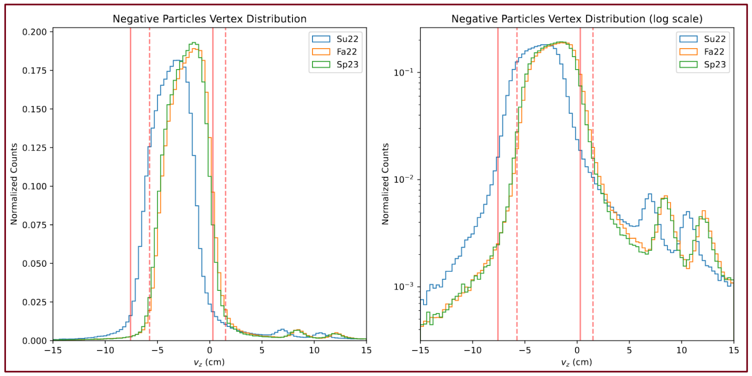

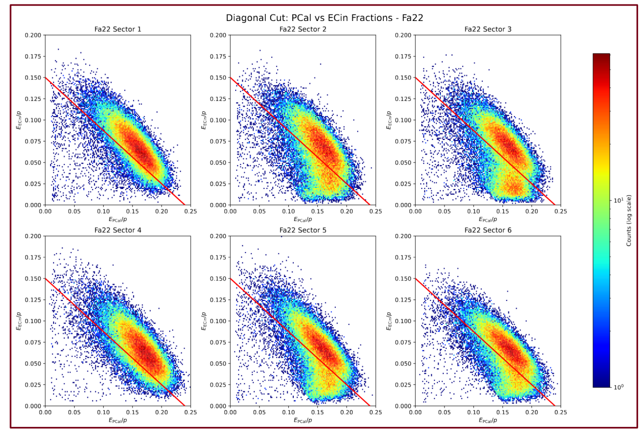

- Vertex cuts
- EB: HTCC signal and P_{CAL} energy deposition
- "Diagonal cut"
- 3σ sampling fraction cut
- Standalone e$^-$ PID document

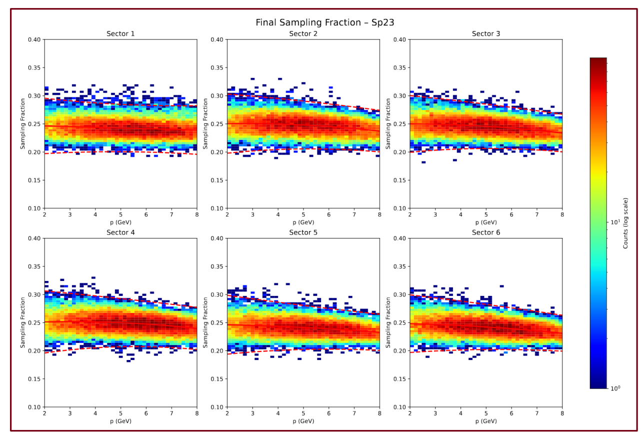

Exclusive Final State

Each x_B-t bin's M_x^2 distribution is fit individually to determine cuts.

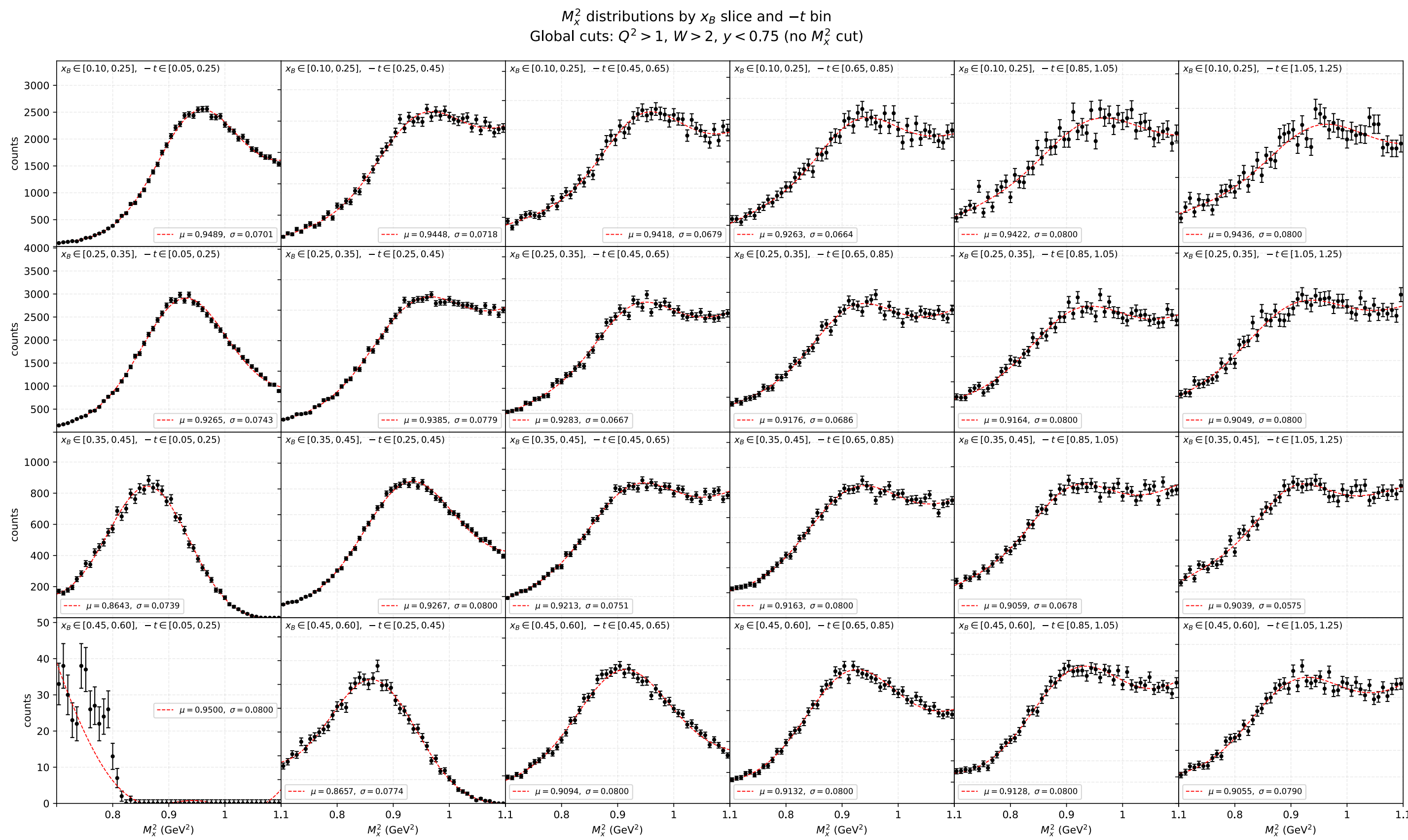

Acceptance Related Effects

- Non-vanishing mean sin(nϕ) indicates possible acceptance related effects.
- Unfolding the data yields with the clasdis MC does not remove these effects (whether because the solenoid “kick” is not fully reflected in MC or because clasdis does not model the exclusive π^+ channel very well).
- Effect is greatly enhanced at lower -t and largely disappears above -t = 1.

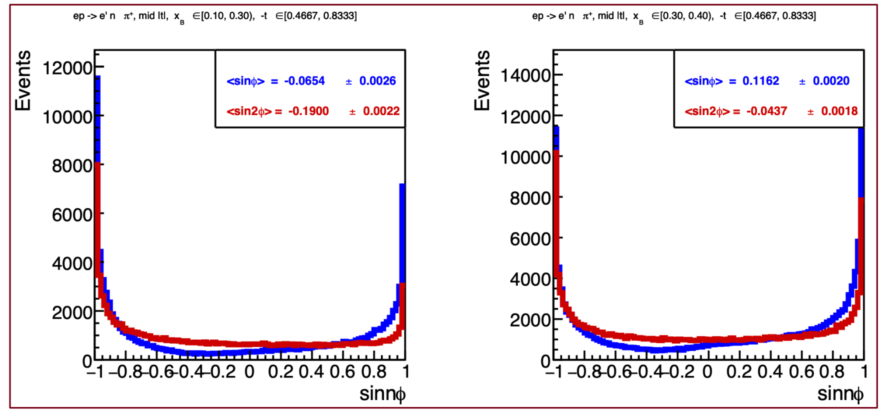

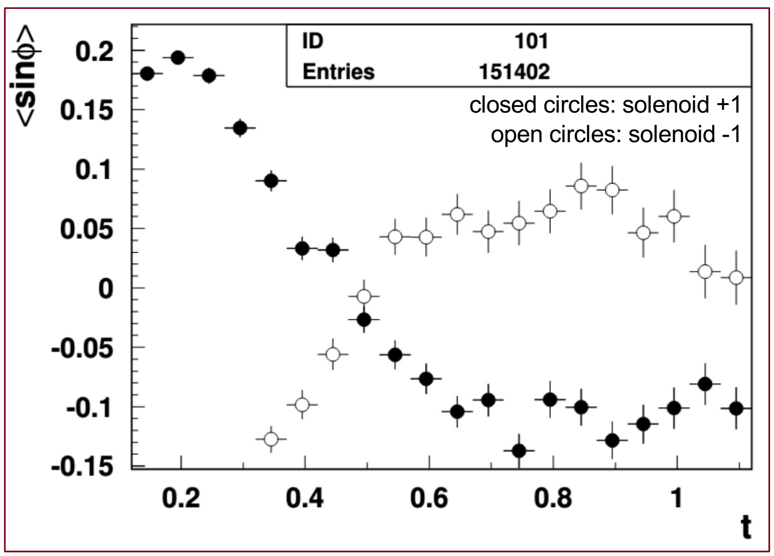

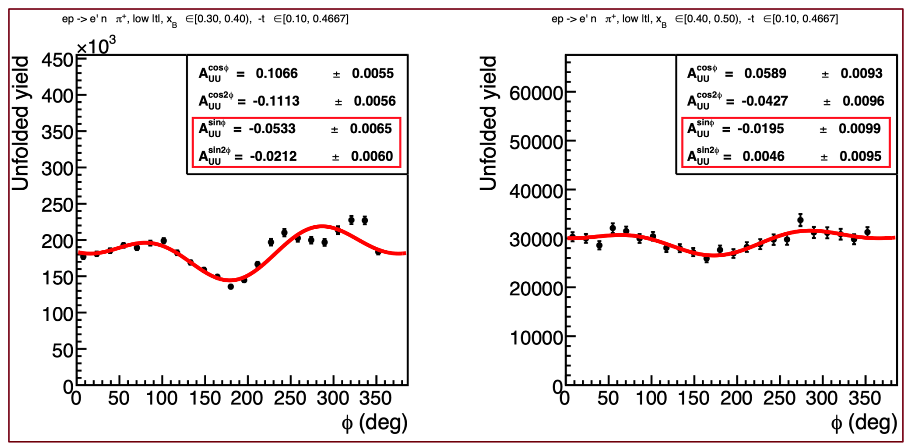

Stability of F_{LU} structure function

1. Extracted from RGA Fa18 Inb data with no unpolarized modulations.
2. Extracted from RGA Fa18 Inb data with the unpolarized $\cos\phi$ and $\cos 2\phi$ modulations included in the fit function.
3. Extracted from RGA Fa18 Inb data with the unpolarized $\cos\phi$ and $\cos 2\phi$ amplitudes fixed to the values extracted from an unfolding of the MC data.
4. Extracted from RGC Fa22 Inb Carbon data with no unpolarizedm odulations.
5. Extracted From RGC Fa22 Inb Carbon data with $\cos\phi$ and $\cos 2\phi$ modulations included in the fit function.
6. Extracted from RGC Fa22 Inb Carbon data with the $\cos\phi$ and $\cos 2\phi$ amplitudes fixed to the values extracted from an unfolding of the MC data.

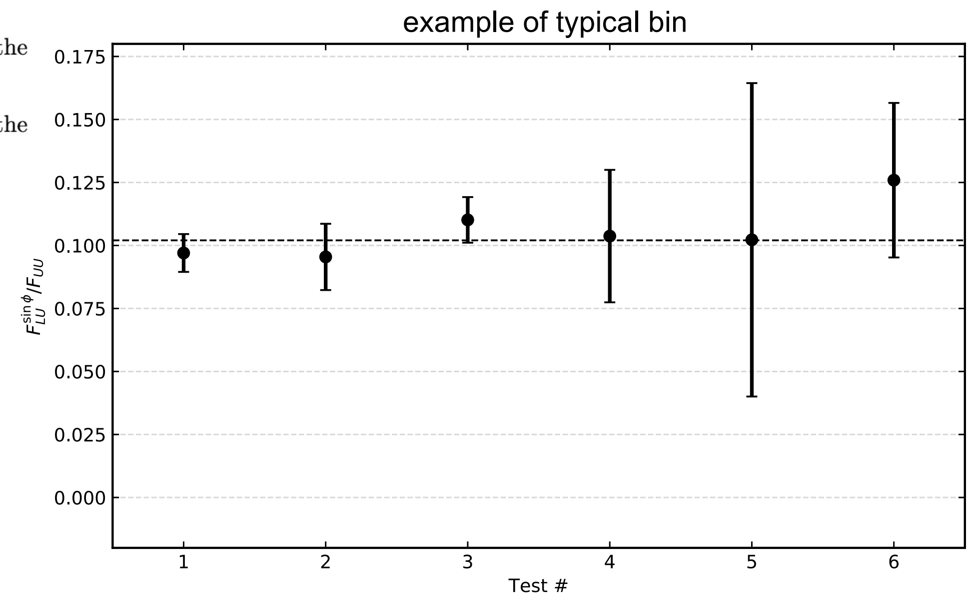

Stability of F_{UL} and F_{LL} structure functions

1. Extracted from RGC Fa22 NH_3 data with all polarized modulations but no unpolarized modulations included in the fit.
2. Extracted from RGC Fa22 NH_3 data with all polarized modulations and $\cos\phi$ and $\cos 2\phi$ unpolarized modulations included in the fit.
3. Extracted from RGC Fa22 NH_3 data with the $F_{LU}^{\sin\phi}$, $F_{UU}^{\cos\phi}$ and $F_{UU}^{\cos 2\phi}$ modulations fixed to values extracted from an independent fit to RGA data in the same kinematic bin.
4. Extracted from RGC Fa22 NH_3 data with the $F_{LU}^{\sin\phi}$ amplitude fixed by an independent fit to RGA data and the $F_{UU}^{\cos\phi}$ and $F_{UU}^{\cos 2\phi}$ modulations fixed to the values extracted from an unfolding of the MC data.
5. Extracted from RGC Fa22 NH_3 data with all polarized and unpolarized modulations allowed to float including two unpolarized sine modulations $A_{UU}^{\sin\phi}$ and $A_{UU}^{\sin 2\phi}$.

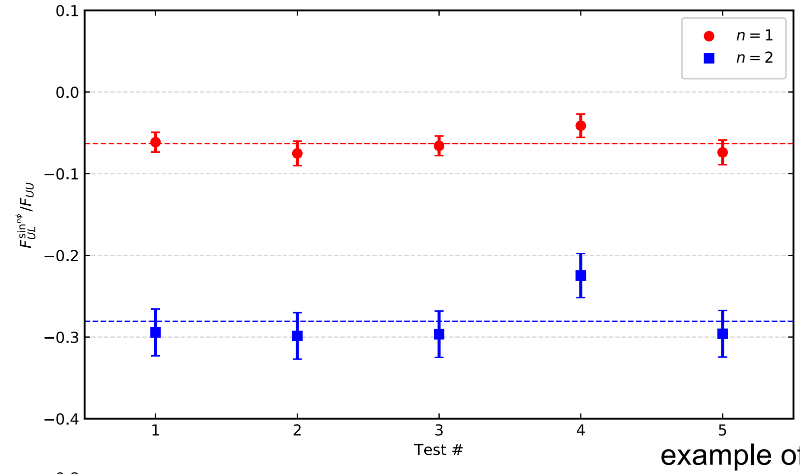

example of typical bin

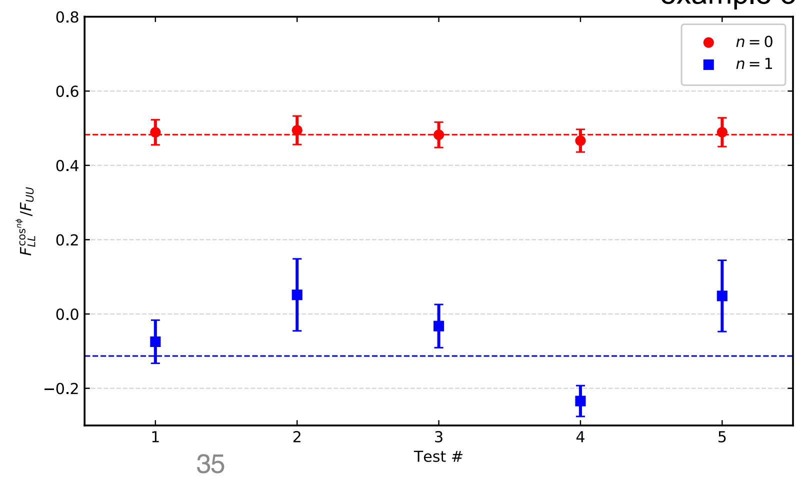

Independence of solenoid setting

RGC Fa22 data with both solenoid settings were investigated separately in each bin and found to return consistent asymmetries.

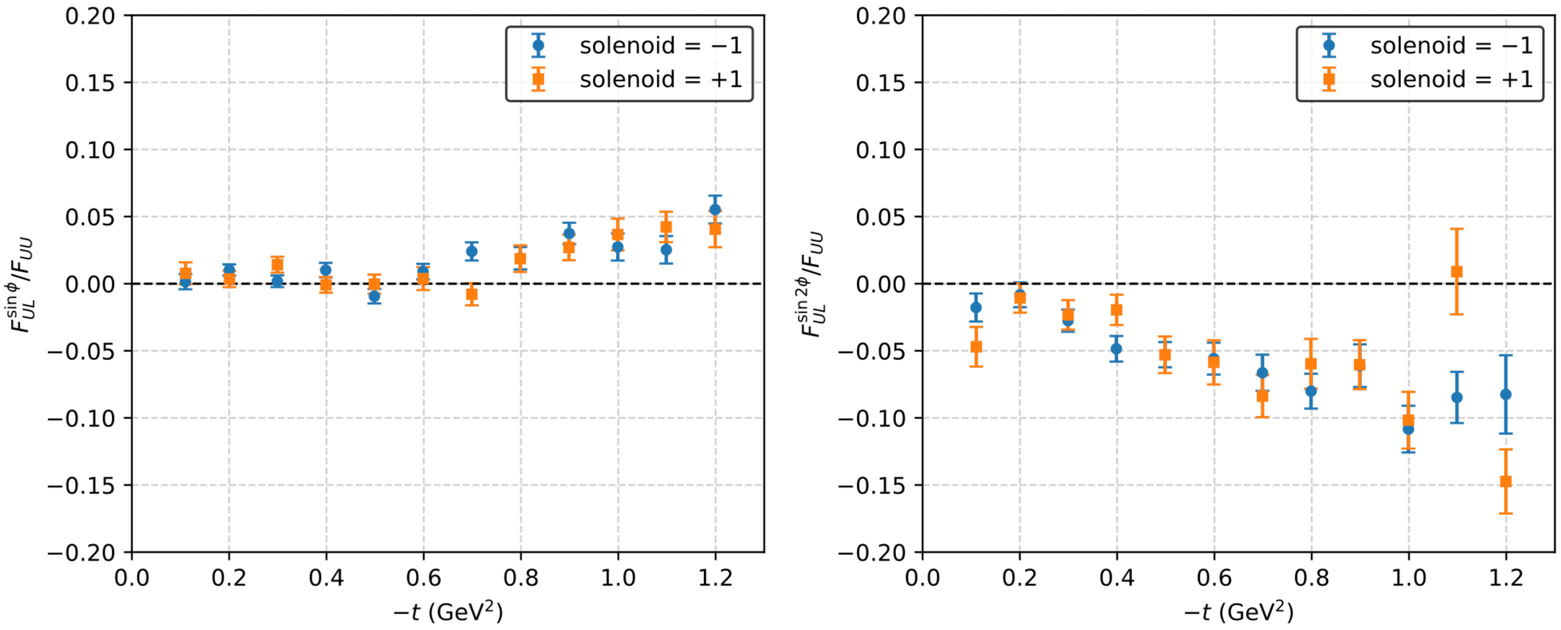

Contribution from tangentially polarized terms

$$\sin\theta_\gamma = \gamma\sqrt{\frac{1-y-\frac{1}{4}y^2\gamma^2}{1+\gamma^2}}$$

- θ_γ defines the angle between the lepton beam-axis and the virtual-photon direction.
- Because the target is longitudinally polarized along the beam it is not completely longitudinally polarized along the direction **q** of the virtual photon.

$$S_{\parallel}^{\gamma} = P_t\cos\theta_\gamma \quad |\vec{S}_T^{\gamma}| = P_t\sin\theta_\gamma$$

- Any non-vanishing tangential polarization can produce UT-type modulations

$$A_{UT}^{\sin\phi}\sin\phi$$

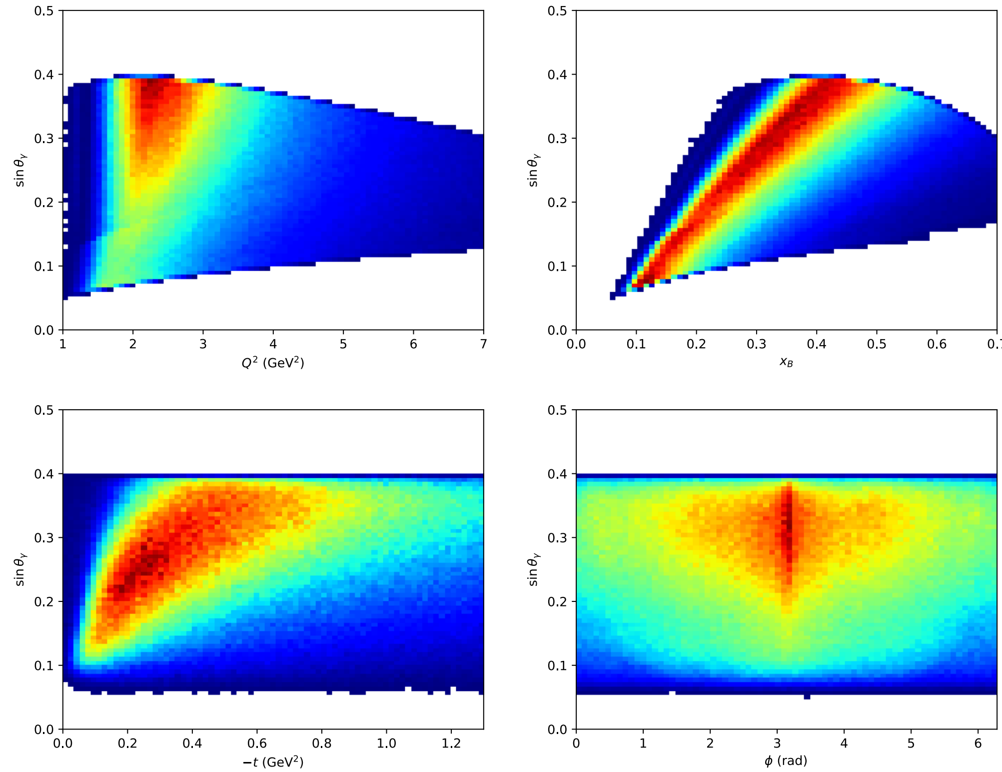

Introduction of "A_{UT}"

- If a $\sin(\theta_\gamma)$ $A_{UT}\sin(\phi)$ term is included directly it will be nearly collinear with the ordinary $\sin(\phi)$ basis.

$$m_i(\phi) \equiv \langle \sin\theta_\gamma \rangle_{\phi_i}$$

$$A_{UL}^{\sin\phi}\sin\phi + A_{UL}^{\sin 2\phi}\sin 2\phi \to A_{UL}^{\sin\phi}\sin\phi + A_{tg}m_i(\phi)\sin\phi + A_{UL}^{\sin 2\phi}\sin 2\phi$$

$$= \left[A_{UL}^{\sin\phi} + A_{tg}m_i(\phi)\right]\sin\phi + A_{UL}^{\sin 2\phi}\sin 2\phi$$

$$m(\phi) \equiv \overline{m} + \delta_m(\phi)$$

- Compute weighted mean and charge weighted width of distribution $\overline{m} = \frac{\sum_i w_i m_i}{\sum w_i}; \quad \sigma_w^2 = \frac{\sum_i w_i (m_i - \overline{m})^2}{\sum_i w_i}$
- Define the centered unitless shape $m_i^c(\phi) = \frac{\delta_m(\phi)}{\sigma_w}; \quad m_i^c(\phi) \equiv \frac{m_i(\phi) - \overline{m}}{\sigma_w}; \quad m_i(\phi) = \overline{m} + \sigma_w m_i^c(\phi)$
- First term renormalizes the $A_{UL}\sin(\phi)$ amplitude, second term carries the genuine shape of the "A_{tg}"
- Rewrite original modulation $m_i(\phi)\sin\phi = [\overline{m} + \sigma_w m_i^c(\phi)]\sin\phi$
- Plug back into TSA $A_{UL}^{\sin\phi}\sin\phi + A_{tg}m_i\sin\phi + A_{UL}^{\sin 2\phi}\sin 2\phi = A_{UL}^{\sin\phi} + A_{tg}\left[\overline{m} + \sigma_w m_i^c(\phi)\right]\sin\phi$

$$= \left[A_{UL}^{\sin\phi} + A_{tg}\overline{m}\right]\sin\phi + A_{tg}\sigma_w m_i^c(\phi)\sin\phi + A_{UL}^{\sin 2\phi}\sin 2\phi$$

Additional ϕ shape from m(ϕ)

- $\sin\theta_\gamma$ generally increases at the edges of ϕ bins.
- If $\sin\theta_\gamma$ had been ϕ-independent there would be no additional modulation effect from the tangential polarization.
- Magnitude of the information about A_{tg} is set by the σ_W (~2-3%).
- If A_{tg} is not fit, A_{UL} shifts by $\overline{m}A_{tg}$

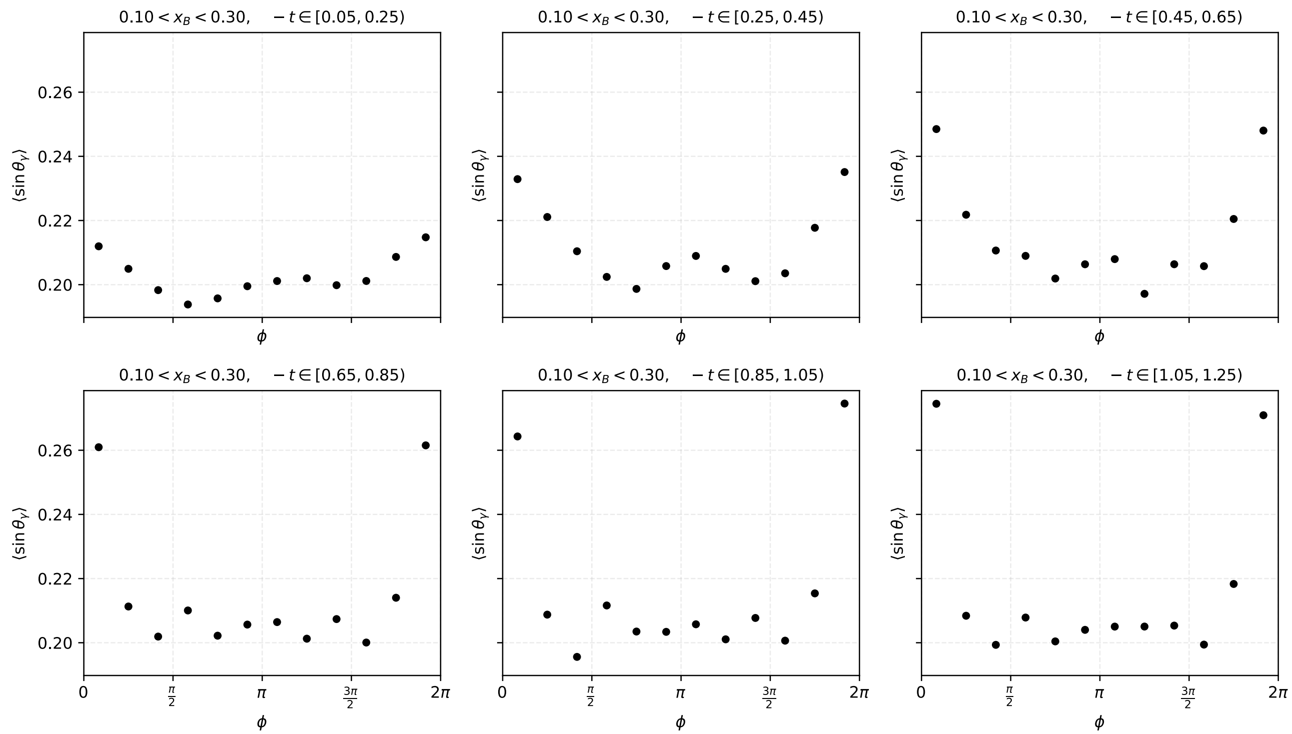

Fits including A_{tg} in TSA

- When included in the fit a small, possibly positive, contribution appears for the A_{tg} term.
- Little to no effect on the regular A_{UL} amplitudes.
- For $\langle\sin\theta_\gamma\rangle \sim 0.23$ and $A_{tg} \sim 0.03$ then $\Delta A_{UL} \sim 0.007$, i.e. a few percent change on the total magnitude.

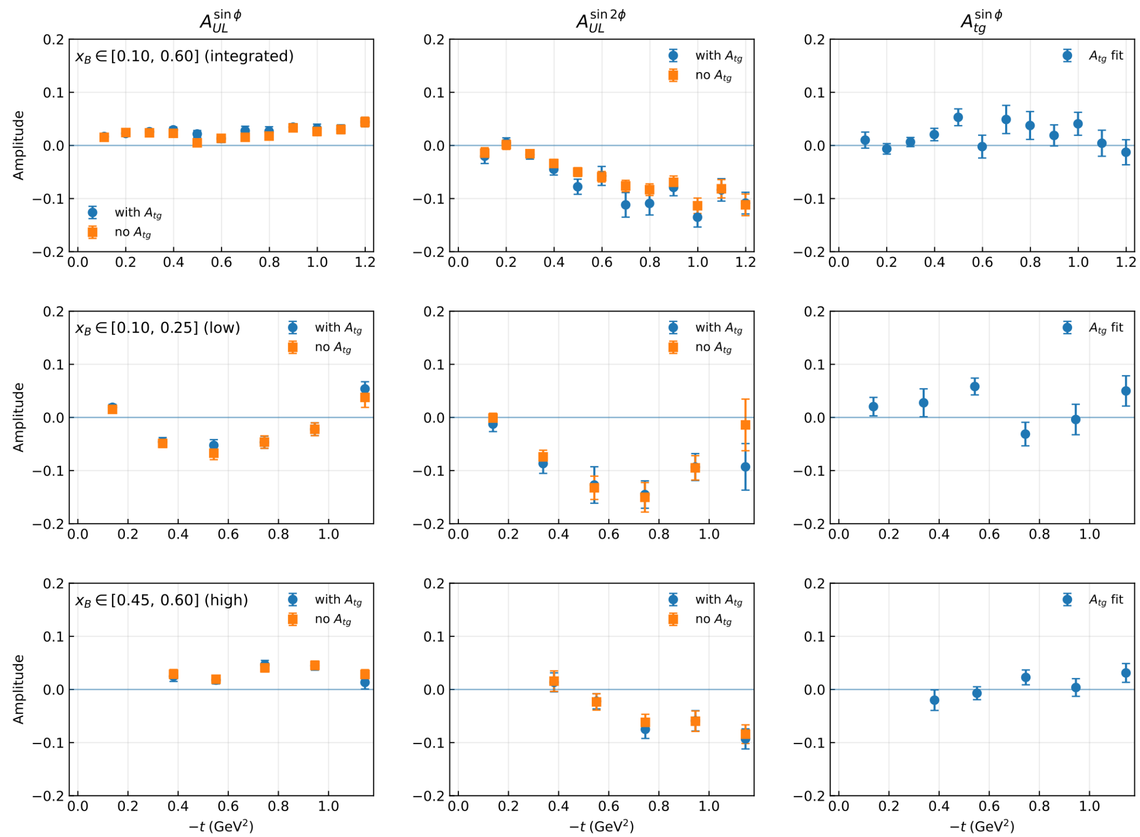

Binned Results (Requested For Release)

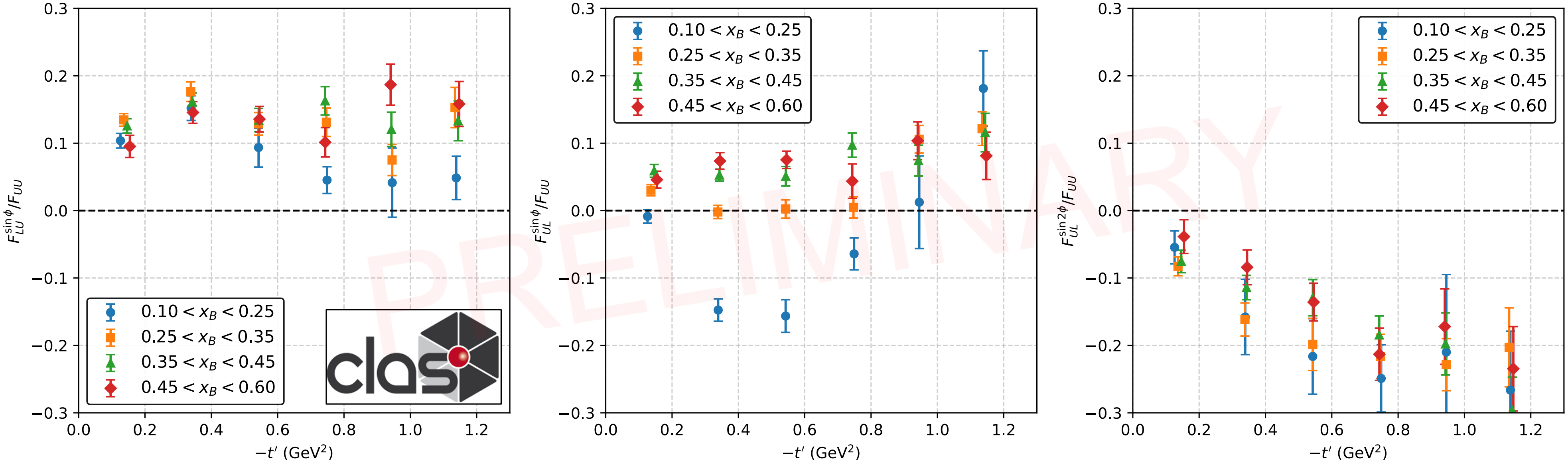

Integrated Asymmetry (Requested For Release)